

DETAIL EXPERIMENTAL TESTING OF UNMANNED AERIAL VEHICLES
ENGINE PERFORMANCE

MOGANARAJ MURUGIAH

Report submitted in partial fulfillment of requirements
for award of the degree of
Bachelor of Mechanical Engineering

Faculty of Mechanical Engineering
UNIVERSITI MALAYSIA PAHANG

JUNE 2013

**DETAIL EXPERIMENTAL TESTING OF UNMANNED
AERIAL VEHICLES ENGINE PERFORMANCE**

MOGANARAJ MURUGIAH

**BACHELOR OF ENGINEERING
UNIVERSITI MALAYSIA PAHANG**

UNIVERSITI MALAYSIA PAHANG
FACULTY OF MECHANICAL ENGINEERING

I certify that the project entitled “*Detail Experimental Testing of Unmanned Aerial Vehicles Engine Performance*” is written by Moganaraj a/l Murugiah. I have examined the final copy of this project and in my opinion, it is adequate in terms of language standard and report formatting requirement for the award of the degree of Bachelor of Engineering. I am here with recommend that it will be accepted in partial fulfillment of the requirements for the degree of Bachelor of Mechanical Engineering.

Dr. Mohamad Firdaus Basrawi
Examiner

(_____)
Signature

SUPERVISOR'S DECLARATION

I hereby declare that I have checked this project and in my opinion, this project is adequate in terms of scope and quality for the award of the degree of Bachelor of Mechanical Engineering.

Signature : _____

Name : Ahmad Basirul Subha Alias

Position : Lecturer

Date :

STUDENT'S DECLARATION

I hereby declare that the work in this thesis is my own except for quotations and summaries which have been duly acknowledged. The thesis has not been accepted for any degree and is not concurrently submitted for award of other degree.

Signature : _____

Name : Moganaraj a/l Murugiah

Id Number : MA 09102

Date :

DEDICATION

To my beloved father and mother

Mr. Murugiah Rajoo

Mdm. Azilatchumi Natchamman

And also siblings

Munesh Murugiah

Yuganesh Murugiah

Thivagar Murugiah

Kavinraj Murugiah

ACKNOWLEDGEMENT

First of all, the deepest sense of gratitude to the God, who guide and gave me the strength and ability to complete this work and fulfill the requirement of BMM 4924 – Final Year Project. Infinite thanks I brace upon Him.

I hereby particularly grateful to my supervisor, Ahmad Basirul Subha bin Alias, for giving me the moral support and encouragement as to complete this piece of work. He was always kind and cooperative. I am also indebted to Assoc. Prof. Dr. Rizalman bin Mamat, Dean of Mechanical Engineering Faculty and my fellow lecturers for giving such knowledge and experience to me since day one in Universiti Malaysia Pahang. They have been my source of inspiration and encouragement in this project.

In the end, I acknowledge the role of my family in the accomplishment of this work. The prayers of my parents and support from my brothers has made all this possible to achieve. Thank you.

ABSTRACT

This project is about detail experimental testing of Unmanned Aerial Vehicles (UAV) engine performance. However, there is no proper selection of test bed available for the performance evaluation, testing and analysis of the UAV propulsion system. This project has two major objectives which are to design and fabricate a test bed for the UAV propulsion system and to conduct detail performance experimentations of the UAV propulsion system run at various speed. In this study, test bed model is designed to test the nitro engine Unmanned Aerial Vehicle (UAV) which is model of Thunder Tiger Pro36 Engine Series of aircraft performance. In addition, six performance parameters are recorded for testing of the engine performance, which are Thrust, shaft brake power, available power, propulsive efficiency, specific fuel consumption and thrust coefficient. Furthermore, the method used in this project is to identify the unknown variables in parameters by using some sensors. The results show that the fabricated test bed can be used to study the engine performance. Specifically, performance parameters are directly proportional to the engine speed. These results show that the performance parameters are increasing along with the speed. In conclusion, the fabricated test bed can be used for the testing of engine performance analysis. Outcomes of this experiment can be successful by using the test bed because it helps to reduce the cost and time for UAV propulsion performances testing.

ABSTRAK

Projek ini adalah menjalankan eksperimen untuk mengkaji dan menganalisis ujian prestasi enjin untuk Pesawat Udara Tanpa Pemandu (PUTP). Walaubagaimanapun, pilihan janakuasa tidak dilaksanakan sepenuhnya dari segi operasi dan prestasi enjin. Projek ini mempunyai dua objektif utama iaitu mencadangkan reka bentuk analisis terperinci dan ujian prestasi Pesawat Udara Tanpa Pemandu (PUTP) sistem dorongan. Dalam kajian ini, model ujian katil diadakan bertujuan untuk menguji enjin nitro iaitu model Thunder Tiger Pro36 Enjin Pesawat dimana enam parameter prestasi telah dikaji seperti Teras, kuasa brek aci, kuasa yang ada, kecekapan pendorongan, penggunaan bahan api brek dan pekali teras. Tambahan pula, kaedah yang digunakan dalam projek ini adalah untuk mengenal pasti pembolehubah yang tidak diketahui dalam parameter dengan menggunakan beberapa sensor. Keputusan menunjukkan bahawa ujian katil direka boleh digunakan untuk mengkaji prestasi enjin. Kesimpulannya, ujian katil boleh digunakan untuk ujian analisis prestasi enjin. Hasil eksperimen ini boleh berjaya dengan menggunakan ujian katil kerana ia membantu untuk mengurangkan kos dan masa untuk ujian prestasi Pesawat Udara Tanpa Pemandu (PUTP) sistem dorongan.

TABLE OF CONTENTS

SUPERVISOR’S DECLARATION	ii
STUDENT’S DECLARATION	iii
DEDICATION	iv
ACKNOWLEDGEMENTS	v
ABSTRACT	vi
ABSTRAK	vii
TABLE OF CONTENTS	viii -xi
LIST OF TABLES	xii
LIST OF FIGURES	xiii
LIST OF ABBREVIATIONS	xiv
CHAPTER 1 INTRODUCTION	
1.1 Project Background	1-2
1.2 Problem Statement	3
1.3 Project Objectives	3
1.4 Project Scope	3
CHAPTER 2 LITERATURE REVIEW	
2.1 Introduction	4
2.2 History Of Unmanned Aerial Vehicle (UAV)	4-5
2.3 UAV Propulsion System	5-8
2.4 Performance Parameters	9
2.4.1 Thrust	9-12
2.4.2 Available Power and Shaft Brake Power	12-13
2.4.3 Propulsive Efficiency	13-15
2.4.4 Brake Specific Fuel Consumption	15-17
2.4.5 Thrust Coefficient	17-18
2.5 PIC Microcontroller	19-20
2.6 Summary	20-21

CHAPTER 3 METHODOLOGY

3.1	Introduction	22
3.2	Flow Chart	23
3.3	Flow Chart Description	24
	3.3.1 Project Introduction	24
	3.3.2 Literature Review	24
	3.3.3 Performance Parameters Analyzes	24
	3.3.4 Preliminary Sketches	24
	3.3.5 CAD Design	25
3.4	Test Bed Modeling Using Solidworks	25
3.5	Material Selection for Test Bed	26
	3.5.1 Base of Wood Plate	26
	3.5.2 Engine Mounting	27
	3.5.3 Slider	27-28
	3.5.4 Nitro Engine	28-29
	3.5.5 Tachometer	29
	3.5.6 Anemometer	30
	3.5.7 Spring and Spring Holder	30-31
	3.5.8 Oil Tank	31
	3.5.9 Servo Set and Electrical Circuit	32
3.6	Fabrication Process	33
	3.6.1 Processes Involved in Fabrication	33
	3.6.2 Steps To Fabricate The Test Bed	33-34
3.7	Experiment Setup	34-35
3.8	Summary	35

CHAPTER 4 RESULT AND DISCUSSION

4.1	Introduction	36
4.2	Thrust	36-38
4.3	Available Power And Shaft Brake Power	38-40
4.4	Propulsive Efficiency	40-41

4.5	Brake Specific Fuel Consumption	42-43
4.6	Thrust Coefficient	44-45
4.7	Summary	45

CHAPTER 5 CONCLUSIONS AND RECOMMENDATIONS

5.1	Conclusions	46-47
5.2	Recommendations	47

REFERENCES		48-49
-------------------	--	-------

APPENDICES

A1	Gantt Chart for FYP 1	50
A2	Gantt Chart for FYP 2	51
A3	Flow Chart of Overall FYP	52
A4	The Raw Data from the Experiment	53
A5	Caluation of Thrust	54
A6	Caluation of Available Power	55
A7	Caluation of Propulsive Efficiency	56
A8	Caluation of Brake Specific Fuel Consumption	57
A9	Caluation of Thrust Coefficient	58
B1	Actual Test Bed Design	59
B2	The Engine and Propeller (Thunder Tiger Pro36)	60
B3	The Base of Test Bed	61
B4	The Pic Microcontroller	62
C1	The Design of Base of Test Bed in Design Software	63
C2	The Design of the Base of Test Bed	64
C3	The Top View of the Test Bed	65
C4	The Front View of the Test Bed	66
C5	The Side View of the Test Bed	67
C6	The Slider Part of the Test Bed	68
C7	The Exploded Drawing of the Test Bed	69

D1	The Orthographic Drawing of the Test Bed's Base	70
D2	The Orthographic Drawing of Slider Part	71
D3	The Orthographic Drawing of Tank Holder	72
D4	The Ortographic Drawing of the Engine Mounting	73
D5	The Ortographic Drawing of the Servo Holder	74
D6	The Ortographic Drawing of the Spring Holder	75
D7	The Ortographic Drawing of the Test Bed	76

List of Tables

Table No.	Title	Page
2.1	The Suggested Propeller Sizes	10
2.2	The Summary of Performance Parameters	11
3.1	The Thunder Tiger Pro36 Series Specification	26
4.1	Tabulated Data for Thrust	38
4.2	Tabulated Data for Available Power And Shaft Brake Power	40
4.3	Tabulated Data for Propulsive Efficiency	41
4.4	Tabulated Data for Brake Specific Fuel Consumption	42
4.5	Tabulated Data for Thrust Coefficient	44

LIST OF FIGURES

Figure No.	Title	page
2.1	Reciprocating Engine	6
2.2	Glow Engine Description	8
2.3	Control Volumes Surrounding A Propeller	10
2.4	Cross-Section of A Propeller	14
2.5	Fuel Tank Placements	16
3.1	Methodology Flow Chart for FYP	23
3.2	Test Bed Design by Using Design Software	25
3.3	Base of The Test Bed	26
3.4	The Nitro Engine Mounting	27
3.5	The Slider Part	28
3.6	The Thunder Tiger PRO36 Series Remote Control Engine	29
3.7	The Tachometer	29
3.8	The Anemometer	30
3.9	The Spring	30
3.10	The Spring Holder	31
3.11	The Oil Tank	31
3.12	The Electrical Circuit	32
3.13	The Servo	32
4.1	Graph of Thrust Vs Speed	37
4.2	Graph of Available Power	39
4.3	Graph of Propulsive Efficiency Vs Speed	41
4.4	Graph of Brake Specific Fuel Consumption Vs Speed	42
4.5	Graph of Thrust Coefficient Vs Speed	44

LIST OF ABBREVIATION

UAV	Unmanned Aerial Vehicle
RC	Radio Controlled
RPM	Revolution Per Minute
BSFC	Brake Specific Fuel Consumption
WW1	World War One
USN	US Navy
dL	Differential lift
dD	Differential drag
PIC	Programmable Interface Controller
FYP	Final Year Project
CAD	Computer-aided Design

CHAPTER 1

INTRODUCTION

1.1 PROJECT BACKGROUND

The term UAV is an abbreviation of Unmanned Aerial vehicle, meaning aerial vehicles which operate without a human pilot. UAVs can be remote controlled aircraft which is flown by a pilot at a ground control station or can fly autonomously based on pre-programmed flight plans or more complex dynamic automation systems. UAVs are commonly used in both the military and police forces in situations where the risk of sending a human piloted aircraft is unacceptable, or the situation makes using a manned aircraft impractical.

Advanced UAVs used radio technology for guidance, allowing them to fly missions and return. They were constantly controlled by a human pilot, and were not capable of flying themselves. This made them much like today's RC model airplanes which many people fly as a hobby.

After the invention of the integrated circuit, engineers were able to build sophisticated UAVs, using electronic autopilots. It was at this stage of development that UAVs became widely used in military applications. UAVs could be deployed, fly themselves to a target location, and either attack the location with weapons, or survey it with cameras and other sensor equipment.

Modern UAVs are controlled with both autopilots, and human controllers in ground stations. This allows them to fly long, uneventful flights under their own control, and fly under the command of a human pilot during complicated phases of the mission.

Currently, UAVs have found many uses in police, military and in some cases in civil application. UAVs are often used in Aerial Reconnaissance to get aerial video of a remote location, especially where there would be unacceptable risk to the pilot of a manned aircraft. UAVs can be equipped with high resolution still, video, and even infrared cameras. The information obtained by the UAV can be streamed back to the control center in real time.

In many cases, scientific research necessitates obtaining data from hazardous or remote locations. A good example is hurricane research, which often involves sending a large manned aircraft into the center of the storm to obtain meteorological data. A UAV can be used to obtain this data, with no risk to a human pilot.

UAVs can be used to carry and deliver a variety of payloads in the logistics and transportation field. Helicopter type UAVs are well suited to this purpose, because payloads can be suspended from the bottom of the airframe, with little aerodynamic penalty.

The importance of this study is to obtain the engine performance parameters such as force, available power, shaft brake power, propulsive efficiency and brake specific fuel consumption from the testing and to suggest suitable powerplant.

The method that has been chosen for this project is by doing experiment to predict the engine performance parameters. This is because by using this method the measurement of engine performance parameters will be more accurate.

1.2 PROBLEM STATEMENT

In this technology era, the UAV propulsion systems are getting popular day by day. Thus, performing various operations on the performances of engine can be difficult since the proper test bed cannot be fully deployed and very limited on the selection. In developing new test bed, many criteria need to be taken into considerations. The criteria that must be taking care are the external design, conceptual design, and preliminary design and detail design.

In this study, the problem that needs to be handled is lack of test bed for performance evaluation, testing, and analysis for UAV propulsion system. There is no proper selection can be made for the test bed in designing new test bed. It is hard to get operational reliable system of UAV propulsion.

1.3 PROJECT OBJECTIVES

For this project, there are two objectives to be achieved as listed below:

- To design and fabricate the test bed for UAV propulsion system experimentations.
- To conduct detail performance experimentations of the UAV propulsion system run at various speed.

1.4 PROJECT SCOPE

The scope for this project are listed as follows:

- Parameters of performance testings. Six parameters are involved which are Thrust, brake power, available power, propulsive efficiency, specific fuel consumptions and thrust coefficient.
- Design PIC microcontroller to control the engine's throttle which increases/decreases rpm of the engine.

CHAPTER 2

LITERATURE REVIEW

2.1 INTRODUCTION

The purpose of this chapter is to revise all the past research, journal, information or study about the UAV, parameters of performance and all others related topic to this project where it will discuss the importance of counter measure and comparison among others research so that it will be used as a guidance in this research.

2.2 HISTORY OF UNMANNED AERIAL VEHICLE (UAV)

Based on GlobalSecurity.org (2008), the history of UAV has already begun as early as before the United States of America enter the World War 1(WW1). Before the WW1, a seaplane that could operate without a pilot onboard is already developed by the US Navy (USN).

The USN has developed and used small plywood UAV in the Pacific for attacking heavily the defended targets. After experiencing heavy losses of aircraft and aircrews by the Army Air Corps, the Aphrodite Projects was introduced. This project uses the old B-17 aircraft loaded with explosive and driven by a pilot. After that, the pilot usage was replaced with radio control of the unmanned aircraft and was use to

send the B-17 to crash into a target. Later on, after WWII, the B-17 were used for testing's the atom bomb in the South Pacific.

In 1964, the Buffalo Hunter which is the US Air Force drone reconnaissance program was under full developed. This drone is use in the Vietnam War as a preprogrammed flight over enemy held territory. Later in 1980, the Pioneer UAV system was introduced where it was used in the Operations Desert Storm which will provide outstanding intelligence and fire support information to the base. While in 2004 due to Iraq War, over 450 UAV was used in the war where it is reported about four teams of 22 soldiers to operate the UAVs in each brigade and until this days, the UAV systems and design is currently ongoing of development process as the military power is being important subjects to every country.

2.3 UAV PROPULSION SYSTEM

There are different views about the precise definition of UAVs (Newcome, 2004). For the purpose of this study, the definition provided by ASTM International was adopted. UAVs are here defined as an airplane, airship, powered lift, or rotorcraft that operates with the pilot in command off-board, for purposes other than sport or recreation (ASTM, 2005). The UAVs are designed to be recovered and reused (ASTM, 2005).

Radio controlled flight, usually referred to as RC, was largely developed by people with interests in both flying and amateur radio, like two early pioneers named Clinton DeSoto and Ross Hull, who flew gliders in the first public exhibition of RC flight (Raine et. all, 2002). He also mention about 1933 the first gasoline powered engines were developed for model airplanes. Although this made the model more realistic it also created the problem of preventing model with its expensive engine simply flying off over the horizon. It was Clinton DeSoto who first envisaged radio as the solution to this problem. Two other names must be mentioned in conjunction with the origins of RC whose is the twin brothers Bill and Walter Good. Walter had an enormous passion for model airplanes while Bill understood radio transmission, and

together in 1937 they built the first RC model plane. That first plane was given the name “Guff,” had an 8-foot wingspan, and weighed 8.5 lbs (Raine et. all, 2002).

In the area of propulsion, the main challenges facing UAV designers are related to the type of engine to employ. The main area of concern for small piston engines (under 50 hp) is reliability and maturity. The trend today is moving towards engines which have obtained certification and are of a high level of maturity. Improvements in UAV propulsion systems are very much dependent on improvements in engines developed for manned aircraft in general aviation, and turbofan / turboprop engines for larger aircraft. The improvements in piston engines are improved power/thrust to weight ratio, lower SFC and noise reduction.

There are several types of engine are used to drive propellers. These engines can be categorized into two major groupings which are internal combustion engines and gas turbine engines (Ward, 1966). Internal combustion engines also known as piston aerodynamic engines. The types of internal combustion piston engines are rotary engines, reciprocating engines, and supercharged reciprocating engines (Ward, 1966). But for this study, the focus only on reciprocating engines.

The engine types commonly used to propel UAVs are four-cycle and two-cycle reciprocating internal combustion engines, rotary engines, and increasingly, electric motors. In some cases, gas turbines are used in UAVs (Fahlstrom & Gleason, 1998).

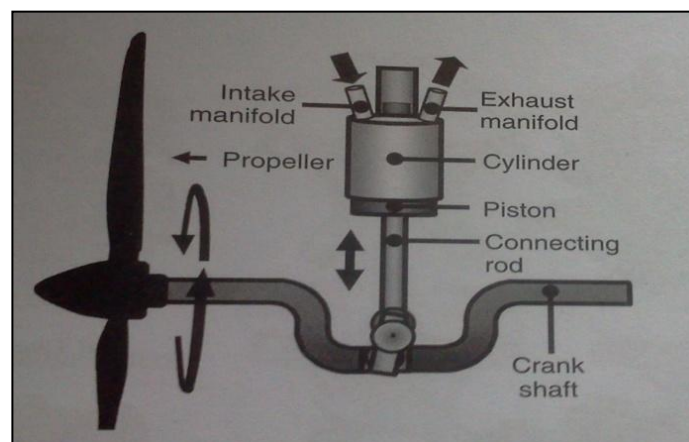


Figure 2.1: Reciprocating engine

Source: Ward, 1966

There are two main propulsion systems used by RC models today which is the internal combustion system (nitro engines) and the electric motors. Combustion engines energy source has so far a higher energy/weight ratio than the batteries used to power the electrics. However, the combustion engines are usually noisier and more prone to oil spillage than the electric motors. There are two types of glow engines which is four-stroke and two-stroke. Two-stroke engines are the most used, mainly because they are simple made, light, easy to operate, easy to maintain, and are usually inexpensive. Two-stroke engines operate at a high RPM and therefore can be quite noisy without a good silencer. As state by (Bird, 2005), when talk about the size of a model airplane, it will usually refer to the size of engine needed to power it (measured in cubic inches). Typically models will be described as a size 20 (which needs a 0.20 HP to 0.36 HP engine), 40 (0.40 HP to 0.53 HP) or 60 (0.60 HP to 0.75 HP). These sizes refer to the capacity in cubic inches, such as, 0.36 cu in, of the most popular 2-stroke glow engines in use and will be adjusted if you change to a different type of engine.

The nitro engine was used in this project was the Max-46LA OS engine. As state by (Hobbico, 2000), the engine have been developed to meet the requirements of beginners and sport flyers which is modern design and having a separate needle-valve unit mounted at rear, where manual adjustment is safely remote from the rotating propeller, they offer the advantages of reliability and easy handling, at lower cost.

Nevertheless, the four-stroke engines also enjoy some popularity, mainly because they produce a lower, more scale-like sound and consume less fuel. They have lower power/ weight ratio and lower RPM, but provide more torque (use larger propellers) than theirs two-stroke counter-parts. However, since the four-stroke engines require high precision engineering and more parts to manufacture, they are usually more expensive. They also need more maintenance and adjustment than the two-stroke, yet they are not too difficult to operate and maintain.

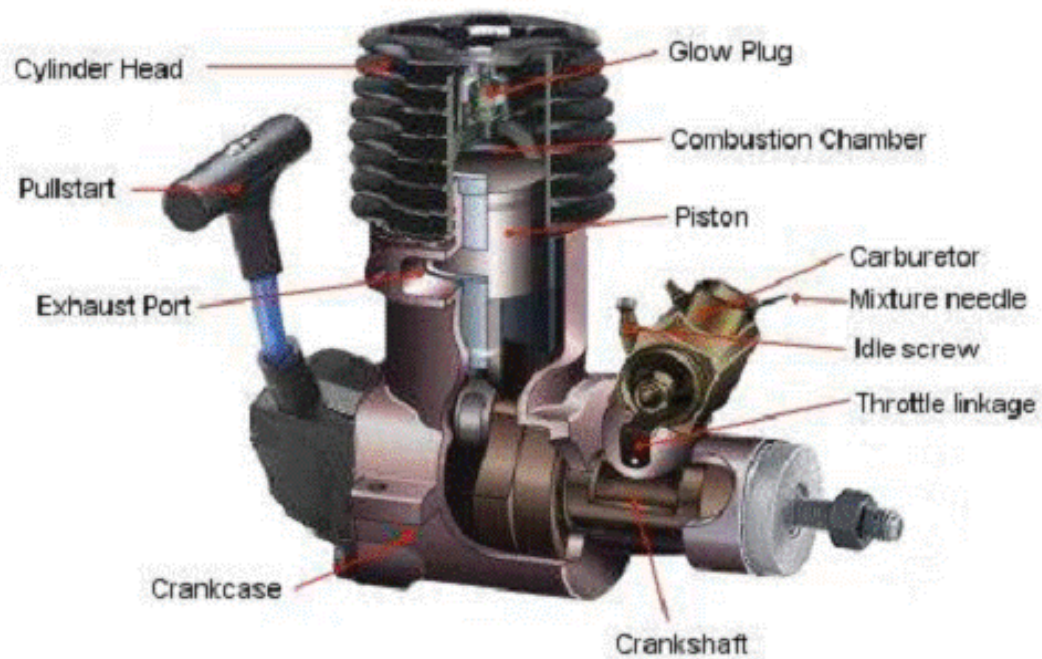


Figure 2.2: Glow engine description

Source: Hobbico, 2000

The glow engine consists of:

1. Glow plug is a type of small internal combustion engine typically used in model aircraft, model cars and similar applications.
2. Combustion chamber is the part of an engine in which fuel is burned.
3. Piston is a component of reciprocating engines.
4. Carburetor is a device that blends air and fuel for an internal combustion engine.
5. Idle screw on carburetor is used to control the amount of air that is allowed into the carburetor continuously, keeping the engine alive when the vehicle is in neutral.
6. Throttle linkage is the mechanism by which the flow of a fluid is managed by constriction or obstruction. An engine's power can be increased or decreased by the restriction of inlet gases.
7. Crankshafts transform the movements of the piston into rotational motion.
8. Crankcase is the housing for the crankshaft.
9. Exhaust Port is an outlet for dissipating the excess heat produced by the large energy reactors.
10. Cylinder head is a crucial part of all combustion engines and cylinder head cracking can result in catastrophic damage to the engine.

2.4 PERFORMANCE PARAMETERS

The parameters of this study are to measure the engine performance such as Available Power, Shaft Brake Power, Brake Specific Fuel Consumption, Propulsive Efficiency, Thrust, and Thrust Coefficient. There is only one type of engine that will be used in this study which is 2-stroke engine. The throttle control of the engine will be used to simulate the engine operating range from idle speed condition until achievable the maximum speed.

2.4.1 Thrust

The forces acting on the airfoil-shaped cross section of a propeller blade are complicated to determine analytically. At first glance, a seemingly simple method of calculating the thrust produced by a propeller blade would be to sum the forces for a small differential radial element (dr) along the length of the blade. It is possible to determine the differential lift (dL) and drag (dD) from the lift and drag coefficients (C_L and C_D) derived from the local airfoil shape and then integrate this equation (Ward, 1966).

However, an ideal approximation of thrust can be derived from the momentum equation by considering a control volume enclosing the airflow accelerated by the propeller (Figure 2.3). This analysis assume that the air flow steadily from a region in front of the propeller (P_o, V_o, ρ_o) to the exit region behind it (P_e, V_e, ρ_e). This method is generally known as the momentum theory (Ward, 1966).

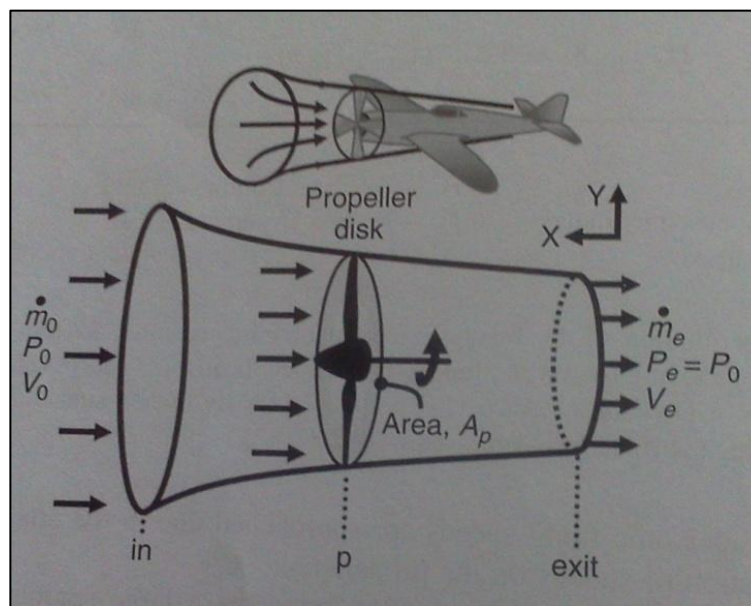


Figure 2.3: Control volumes surrounding a propeller

Source: Ward, 1966

It is assumed that flow outside of the propeller stream tube does not experience any change in total pressure. Therefore the pressure terms everywhere are balanced, so the only force on the control volume is due to changes in longitudinal (x-direction) momentum fluxes across its boundaries. Propeller was known by modelers, as “props”, the sole purpose of this important and often overlooked piece of equipment is to pull (and sometimes push) the airplane through the air (Tressler, 2008). The suitable type and size of propeller is important to draw maximum power output from the Remote control engine. As the ideal propeller diameter, pitch and blade area vary according to the size, weight and type of model, final propeller selection will require in flight experimentation. The suggested propeller sizes are given in the table (Hobbico, 2000).

Table 2.1: The suggested propeller sizes for different engine ratings.

LA Series	Running-in	Trainer & Sport
40 LA	11×5	10×6-7, 10.5×6, 11×5-6
46LA	11×6	11×6-7
65LA	12×6	12×7-8, 13×6-8

There are several types of propellers in use on model airplanes. They include two, three, and four blade types. By far, the most popular propeller for a trainer plane is a two blade type made of wood or plastic (Tressler, 2008). Most used are plastic propellers. Propellers are sized using two numbers; diameter and blade pitch. A very common prop size for a 40 to 46 trainer engine is a 10-7. The first number is the diameter of the propeller in inches. The second is the blade pitch expressed as a number representing the theoretical distance the airplane travels forward for each revolution of the propeller.

In the example propeller, the 10-7 indicated a 10 inch propeller that moves the airplane forward 7 inches per revolution. Model engine propellers range in overall diameter from 5 inches up through and including. The main advantage of plastic over wood primarily is the increased durability of plastic. Chances are good to break a wood propeller more easily during initial flight training.

Most important thing while handling the propeller is never touch, or allow any object to come into contact with the rotating propeller and do not crouch over the engine when it is running (Hobbico, 2000). The rotating propeller will produce thrust as shown in Figure 2.3. The ideal thrust equation for piston aerodynamics engines as shown in Eq. (2.1).

$$F_N = \dot{m}_e V_e - \dot{m}_o V_o = \dot{m}(V_e - V_o) \quad (2.1)$$

Where,

\dot{m}_e is mass flow rate at exit of propeller (kg/s).

\dot{m}_o is mass flow rate at inlet of propeller (kg/s).

V_o is air velocity at inlet of propeller (m/s).

V_e is air velocity at exit of propeller (m/s).

For this study, assume that the force is equal to the spring constant times the distance the spring is elongated from its equilibrium position in meters. The force can be measure by the simple equation known as Hooke's Law as Eq. (2.2).

$$F = kX \quad (2.2)$$

Where,

k is the spring constant(N/m).

X is elongation of spring during parameters testing (m).

Hence, in order to measure the thrust exert by propeller while the engine start, the spring was placed on between the rear slider and spring's stand to measure the force by measure the elongation of the spring while force from the propeller pulls the slider toward. The value of force can be calculated because the spring constant can be measured.

2.4.2 Available Power and Shaft Brake Power

A propeller generates thrust by inducing a low pressure region in front of itself and a high pressure region behind itself ($P > P_o$). (A detail kinematic model that describes all the aerodynamics forces involved is very complex and beyond the scope of this study.) The air pressure downstream of the propeller eventually returns to free stream conditions, but just behind the propeller the air velocity is greater than the free stream velocity (V_o). This is because the propeller has done work on the airflow (Ward, 1966).

In actual piston aero engines the shaft brake power cannot be perfectly transmitted to the propeller as available power, because of losses associated with the compressibility of air. The available power is the rate that useful work is done. The equation of available power can be simplified as shown in Eq. (2.3).

$$\dot{W}_A = F_N V_o \quad (2.3)$$

Where,

F_N is the thrust of the engine (N).

V_o is air velocity at inlet of propeller (kg/s).

The shaft brake power is simply equal to the power expended by the propeller and imparted to the fluid. This is simply the rate of change in the kinetic energy of the flow passing through it. The equation of shaft brake power can be simplified as shown in Eq. (2.4).

$$\dot{W}_B = \dot{m} \left[\left(\frac{V_e^2}{2} - \frac{V_o^2}{2} \right) \right] \quad (2.4)$$

Where,

\dot{m} is mass flow rate of air at propeller (kg/s).

V_o is air velocity at inlet of propeller (m/s).

V_e is air velocity at exit of propeller (m/s).

The unknown that needed to solve the equation is the speed of the air in front and rear the propeller. Hence, the anemometer is used to get the value of V_o and V_e in front and rear the propeller at specific engine speed so that the available and shaft brake power data can be obtain.

2.4.3 Propulsive Efficiency

Aircraft propellers generally consist of two to six propeller blades as discussed in previous section. The number of blades needed depends upon the power of the engine. More powerful engines require a greater number of blades to efficiently convert this power into thrust. Unlike marine propellers, all aircraft propeller blades are arranged radials perpendicular to the axis of rotation and consist of a set of airfoil-shaped cross section. The term station is used to define radial positions (r) along a

propeller from root (or hub) to tip. At any station the blade cross section has an airfoil shaped, but this shape may vary in outline at different stations. A wing is fixed (with respect to the airplane) and only experiences the relative free-stream flow of the air. A propeller is not fixed because it rotates. Therefore a propeller experiences an oncoming flow of air that is the vector sum of the airplane's velocity (also called the free-stream velocity, V_o) and the propeller rotational velocity (Ward, 1966).

As state by (Ward, 1966), Figure 2.4 illustrates the airfoil cross section of a propeller. Early propellers generally used airfoil cross sections that were similar to those used in wings. But as new higher speed aircraft were developed these airfoils proved to be inefficient. This is because the local velocity acting on specific propeller section is higher than the speed of the aircraft. This can cause flow separation or the formation of shock waves in the propeller airstream. This phenomenon known as a compressibility burble causes thrust losses and additional drag.

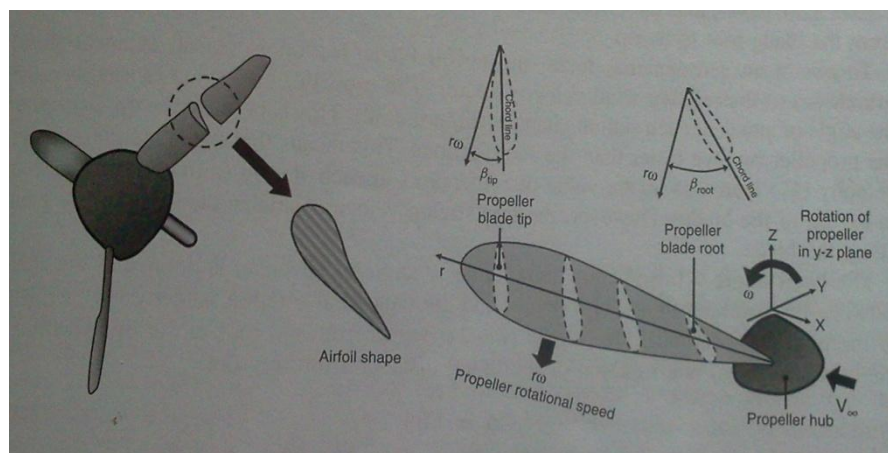


Figure 2.4: Cross-Section of a propeller

Source: Ward, 1966

It is useful to define a propeller efficiency (η_{prop}) that relates the fraction of shaft brake power delivered to the propeller and converted into propeller thrust power (available power) as shown in Eq. (2.5).

$$\eta_p = \frac{F_{N,prop} V_o}{\dot{W}_B} = \frac{\dot{W}_A}{\dot{W}_B} \quad (2.5)$$

Where,

F_N is force exerted by propeller (N).

V_o is velocity of air at inlet of propeller (m/s).

\dot{W}_A is available power (Nm/s).

\dot{W}_B is shaft brake power (Nm/s).

The available and shaft brake power can be calculated as described in previous section. Then it means the value of propulsive efficiency also can be calculated because every value needed is available and can be found by solving the mathematical equation. There is no difference between the propeller efficiency (η_{prop}) and propulsive efficiency (η_{prop}) because as stated by (Ward, 1966), the propeller efficiency (η_{prop}) is generally equal to the propulsive efficiency (η_{prop}) for aero piston engines.

2.4.4 Brake Specific Fuel Consumption

Brake specific fuel consumption (BSFC) is a measure of the efficiency of an internal combustion engine. The term "specific fuel consumption" refers to the amount of fuel used normalized to the amount of power generated, which gives you an efficiency at certain operating point of the engine. All glow engines require a special fuel, called glow fuel. It consists of methanol as base, with some amount of nitro methane to increase the energy and pre-mixed oil into the fuel, which lubricates and protects the engine parts. Most glow engines will come with a manufacturer's recommendation for fuel/oil mix with a type and percentage of oil specified. This is probably applicable to running in the engine and should comply with the manufacturer's recommendation.

Two-stroke engines operate by igniting the fuel in its combustion chamber once every turn of its crankshaft. The fuel is mixed with air at the carburetor and forced into the cylinder during the down movement of the piston (1st stroke). While the piston moves up, the mixture is compressed and when the piston reaches the top, the glow plug ignites the compressed gases, forcing the piston down (2nd stroke). On the way down exhaust gases escape through the exhaust port while the fuel mixture enters the cylinder again.

In a four-stroke engine the fuel/air mixture enters the combustion chamber during the down movement of the piston through a valve operated by the camshaft (1st stroke). When the piston moves up, the valve closes and the mixture is compressed (2nd stroke). When the piston reaches the top, the glow plug ignites forcing the piston down (3rd stroke). On the next up movement of the piston, a second valve opens and allows the exhaust gases to escape (4th stroke). The piston moves down and the fuel mixture enters the combustion chamber again, repeating the 1st stroke.

The fuel tank size and location will affect the engine operation. A typical fuel tank placement is shown on the picture below:

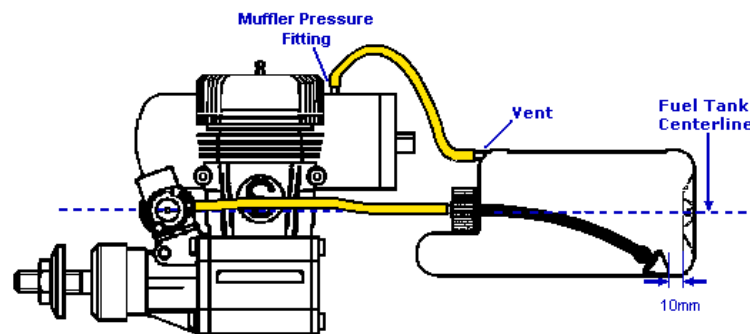


Figure 2.5: Fuel tank placements

Source: Hobbico, 2000

As stated by (Hobbico, 2000), when the engine is in the upright position, the fuel tank's centerline should be at the same level as the needle valve or no lower than 1cm, (3/8 in) to insure proper fuel flow. A too large fuel tank may cause the motor to run "lean" during a steep climb and "rich" during a steep dive. Normal tank size for engines between 3.5cc (0.21 HP) and 6.5cc (0.40 HP) is 150 - 250cc.

Model engine fuel is poisonous. Never allow it come into contact with the eyes or mouth. Always store it in a clearly marked container and out of the reach of children. Model engine fuel is also highly flammable. Keep it away from open flame, excessive heat, sources of sparks, or anything else which might ignite it (Hobbico, 2000).

The type of specific fuel consumption that is commonly used as a figure of merit in piston aero engines is called the brake specific fuel consumption (BSFC). It is defined as the rate of fuel consumption divided by the rate of shaft brake power production (Ward, 1966). The equation for brake specific fuel consumption can be state as shown in Eq. (2.6).

$$\text{BSFC} = \frac{\dot{m}_{\text{fuel}}}{\dot{W}_B} = \eta_p \frac{\dot{m}_{\text{fuel}}}{\dot{W}_A} \quad (2.6)$$

Where,

\dot{m}_{fuel} is mass flow rate of fuel (kg/s).

η_p is propulsive efficiency.

\dot{W}_A is available power (Nm/s).

\dot{W}_B is shaft brake power (Nm/s).

The unknown that needed to get the value of BSFC is the mass flow rate of fuel. The mass flow rate of fuel can be measure by the mass of fuel divided to the time taken while run the nitro engine. Then the mass flow rate of fuel that just calculated is used again to calculate the value of BSFC. From the definition of BSFC it is clear that lower values represent more fuel efficient engines.

2.4.5 Thrust coefficient

Thrust coefficient (C_f) is an non-dimensional expression of thrust for a piston aero engine. It is defined as :

$$C_f = \frac{F_N}{\rho \eta_{\text{prop}}^2 d^4} \quad (2.7)$$

Where,

C_f is Thrust coefficient.

F_N is Thrust (N).

ρ is density (kg/m³).

d is diameter (m).

Table 2.1 shows the summarized of the equations that are used in this study and the unknown parameters to be finding from the test bed.

Table 2.2: The Summary of the Performance Parameters

No.	Performance Parameters	Equation	Parameter to be measured
1	Thrust	$F = kX$	X
2	Available Power	$\dot{W}_A = \dot{m}v_o(v_e - v_o) = F_N v_o$	V_e, V_o
3	Shaft Brake Power	$\dot{W}_B = \dot{m} \left[\left(\frac{v_e^2}{2} - \frac{v_o^2}{2} \right) \right]$	V_e, V_o
4	Propulsive Efficiency	$\eta_p = \frac{F_{N,prop} v_o}{\dot{W}_B} = \frac{\dot{W}_A}{\dot{W}_B}$	V_o
5	Brake Specific Fuel Consumption	$BSFC = \frac{\dot{m}_{fuel}}{\dot{W}_B} = \eta_p \frac{\dot{m}_{fuel}}{\dot{W}_A}$	\dot{m}_{fuel}
6	Thrust Coefficient	$C_f = \frac{F_N}{\rho \eta_{prop}^2 d^4}$	η_{prop}, d

Where;

X is displacement of spring during parameters testing (m).

V_e is exit velocity (m/s).

V_o is entrance velocity (m/s).

\dot{m}_{fuel} is mass flow rate of fuel (kg/s).

η_{prop} is propeller revolution per second (rps).

d is diameter of circular disk formed by rotating propellers (m).

2.5 PIC MICROCONTROLLER TO CONTROL THE ENGINE THROTTLE

PIC microcontrollers is the Programmable Interface Controllers. PIC Microcontrollers are electronic circuits that can be programmed to carry out a vast range of tasks. They can be programmed to be timers or to control a production line and much more. They are found in most electronic devices such as alarm systems, computer control systems, phones, in fact almost any electronic device. Many types of PIC microcontrollers exist, although the best are probably found in the GENIE range of programmable microcontrollers. These are programmed and simulated by Circuit Wizard software. PIC Microcontrollers are relatively cheap and can be bought as pre-built circuits or as kits that can be assembled by the user. The program inside PIC will need a computer to run software, such as Circuit Wizard, allowing you to program a PIC microcontroller circuit. A fairly cheap, low specification computer should run the software with ease. The computer will need a serial port or a USB port. This is used to connect the computer to the microcontroller circuit. Software such as, Genie Design Studio can be downloaded for free. It can be used to program microcontroller circuits. It allows the programmer to simulate the program before downloading it to a PIC microcontroller IC simulating the program on screen, allows the programmer to correct faults and to change the program.

The software is quite easy to learn, as it is flow chart based. Each 'box' of a flow chart has a purpose and replaces numerous lines of text programming code. This means that a program can be written quite quickly, with fewer mistakes.

PIC Microcontrollers are quickly replacing computers when it comes to programming robotic devices. These microcontrollers are small and can be programmed to carry out a number of tasks and are ideal for school and industrial projects. A simple program is written using a computer, it is then downloaded to a microcontroller which in turn can control a robotic device.

The advantages of PIC architectures are listed below:

- Small instruction set to learn.
- RISC architecture.
- Built in oscillator with selectable speeds.
- Easy entry level, in circuit programming plus in circuit debugging PICkit units.
- Inexpensive microcontrollers.
- Wide range of interfaces.

The limitations of PIC architectures are listed below:

- One accumulator.
- Register-bank switching is required to access the RAM of many devices.
- Operations and register are not orthogonal and some instruction can address RAM and/or immediate constants, while others can only use the accumulator.
- The following stack limitations have been addressed in the PIC18 series, but still apply earlier cores:
- The hardware call stack is not addressable, so preemptive task switching cannot be implemented.
- Software-implemented stacks are not efficient, so it is difficult to generate and support local variables.

2.6 SUMMARY

In this chapter, the discussion is more on introduction about UAV propulsion systems for two-stroke and four-stroke engine (remote control engine). The detail on type of engines, thrust, combustion, and propeller design will be used. From that we can determine the engine performance parameters from output of engine type such as thrust, available power, shaft brake power, propulsive efficiency, and brake specific fuel consumption by solving mathematical equations. The unknown variables can be obtained from data given by the apparatus reading such as spring, anemometer, and tachometer that are installed within the test bed design.

Besides that, is Programmable Interface Controller (PIC) designed to control engine throttle. PIC programming designed to control the servo motor. Servo motor is controlling the throttle for increase and decrease the engine speed.

CHAPTER 3

METHODOLOGY

3.1 INTRODUCTION

The objective of this project can be achieved by preparing an organized methodology. This ensures the project is capable to be completed on time. This chapter will explain the details about the methodology progress during Final Year Project 1 and 2. This chapter will list all the methods that were included and relevant to complete this project. The title “Detail Experimental Testing of Unmanned Aerial Vehicles Engine Performance” was given by the faculty at the beginning of the semester. The literature study that is related to this topic has been carried out in Chapter 2.

This section will briefly describe the ways to fabricate the test bed from the equipments and parts with the material selection for making test bed to determine the best and accurate result for this study. The test bed modeling using Design Software also will be shown later in this section. Besides that, this section also briefly describes the way how the study being conduct, which is by doing experiment to obtain data from test bed.

The variables and performance parameters also will be explained other than problem setup. Thus, all the data values from the experiment will be obtain for nitro engine type and finally will be able to suggest the suitable test bed.

3.2 FLOW CHART

The flow chart of project is shown below:

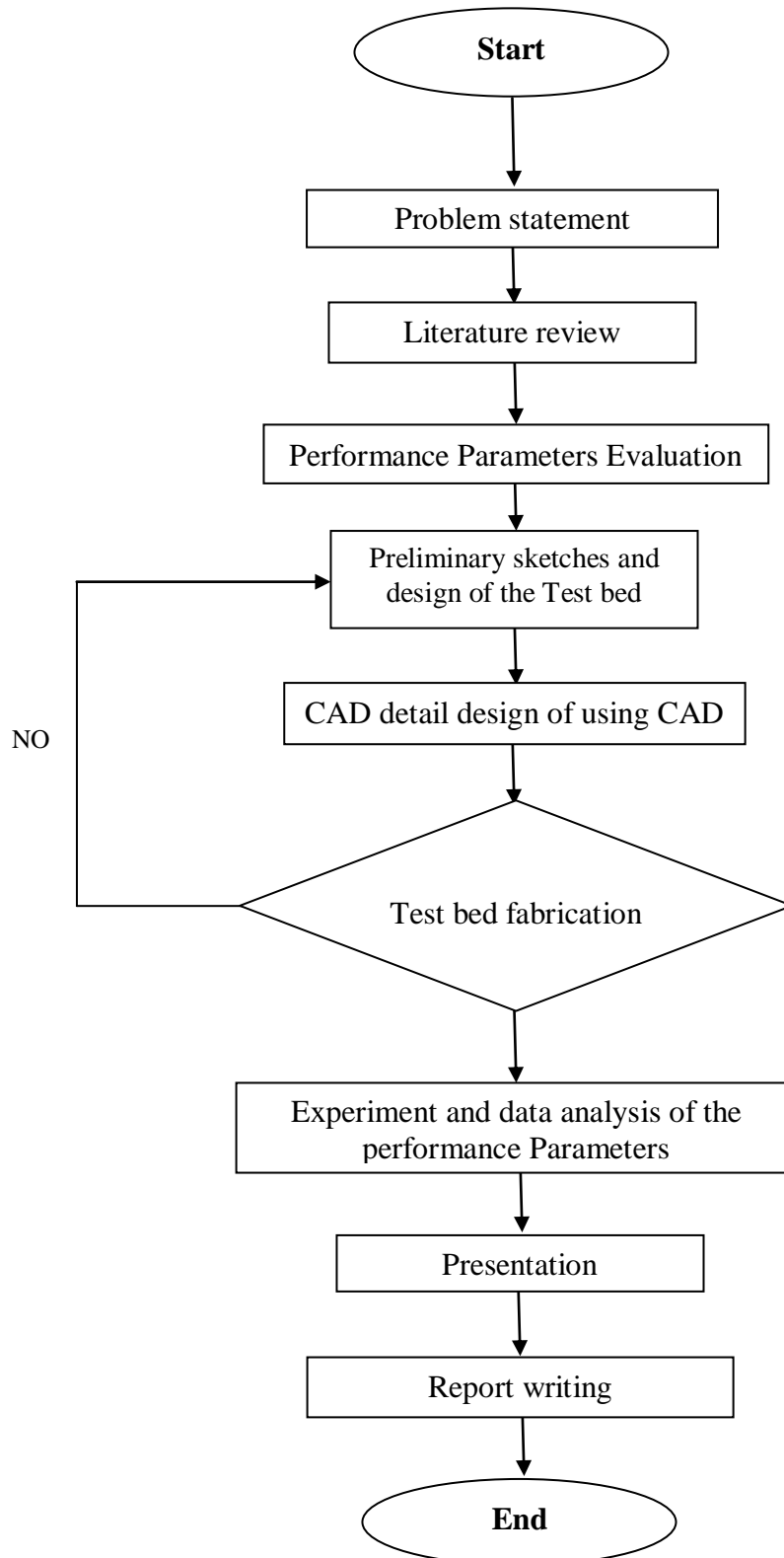


Figure 3.1: Methodology flow chart for FYP

3.3 FLOW CHART DESCRIPTION

3.3.1 Project Introduction

The project started with the title confirmation by the faculty. Upon discussion with the supervisor of the project, the main contents were determined. Project objective is the most important part in this project. By the determination of the objective, the project will clearly see what has to be done from the beginning. This is very important so that the target objective can be achieved from the starting. The scopes of this project can be done after determine the objective. This will help the project to progress smoothly and can be successful.

3.3.2 Literature Review

This project is continued with literature review, research from the internet, company websites, books and journals about the title. This stage is very important while making literature review because the performance parameters and Programmable Interface Controllers (PIC) programming must be study. In this part, design of test bed, function of PIC and importance of cooler system all will be explained. The literature study was added from the beginning of this project so that all the latest information will be updated from time to time.

3.3.3 Performance Parameters analyzes

Next, choose some performance parameters and do some research. Finally six performance parameters were selected for performance testing.

3.3.4 Preliminary Sketches

Several sketches were made and picked as the main references in the project.

3.3.5 CAD Design

After all the sensors are placed in one test bed in preliminary sketches and satisfy with the preliminary, the next step is to design the test bed in CAD and also the sensors in test bed.

3.4 TEST BED MODELING USING DESIGN SOFTWARE

This section will describe the details of the test bed modeling by using Design software. Design software is a 3D mechanical CAD (computer-aided design) program. Building a model in design software usually starts with a 2D sketch (although 3D sketches are available for power users). The sketch consists of geometry such as points, lines, arcs, conics (except the hyperbola), and splines. Dimensions are added to the sketch to define the size and location of the geometry. Relations are used to define attributes such as tangency, parallelism, perpendicularity, and concentricity. The parametric nature of design software means that the dimensions and relations drive the geometry, not the other way around. The dimensions in the sketch can be controlled independently, or by relationships to other parameters inside or outside of the sketch.

The parts of the test bed are made one by one before assembly it according to actual size. The assembly design as shown in Figure 3.2.

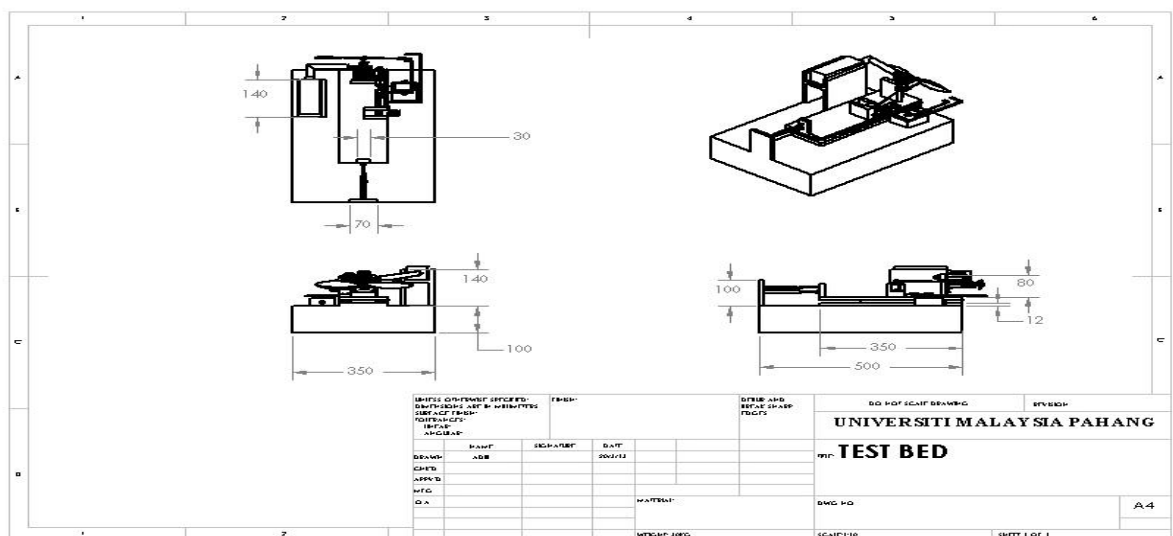


Figure 3.2: The test bed design by using Design Software

3.5 MATERIAL SELECTION FOR TEST BED

It is important to choose the suitable materials to build the test bed because it will affect the result of the project either the measurement become inaccurate or not applicable.

3.5.1 Base of Wood Plate

The wood plate is used as base of the test bed because it has the ability to absorb the vibration of the running engine. Vibration is a mechanical phenomenon whereby oscillations occur about an equilibrium point. The oscillations may be periodic such as the motion of a pendulum or random such as the movement of a tire on a gravel road. The lower rate of vibration will defend the oil in oil tank to be unstable and may give effect to the running engine. Moreover, the wood plate weight is heavy and able to avoid the test bed to move from its spot.

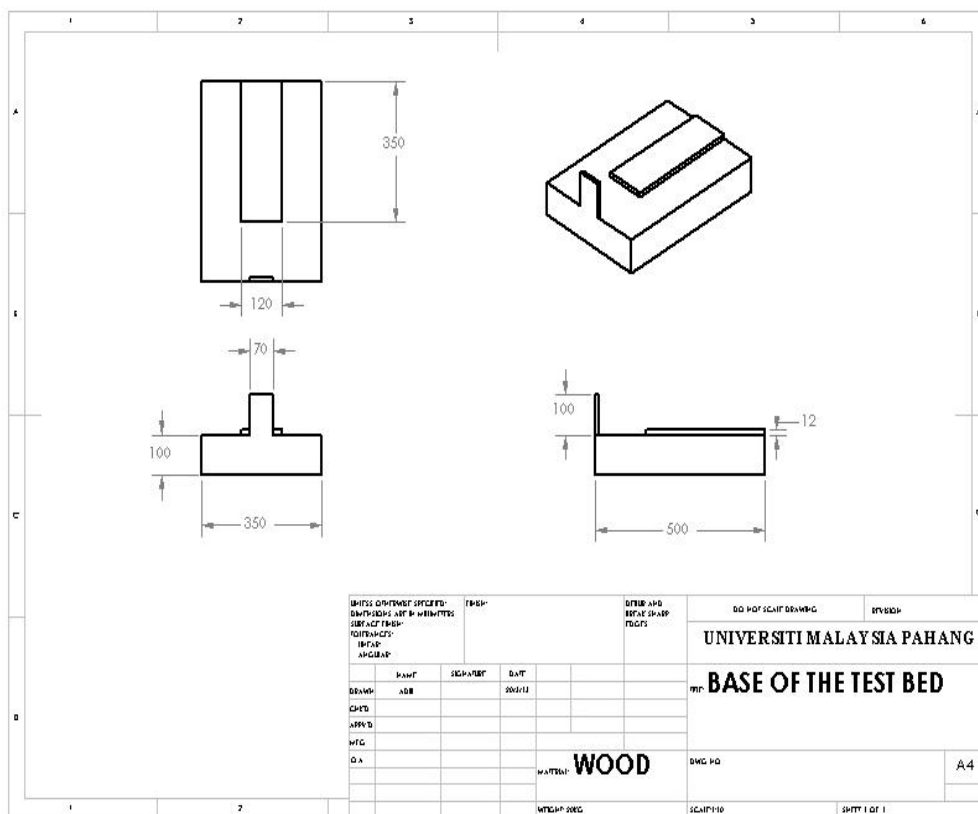


Figure 3.3: Base of the test bed

3.5.2 Engine Mounting

The engine mounting will be made from the wood while spring holder will be made from aluminum. This ensures that it will stand from corrosion and last longer.

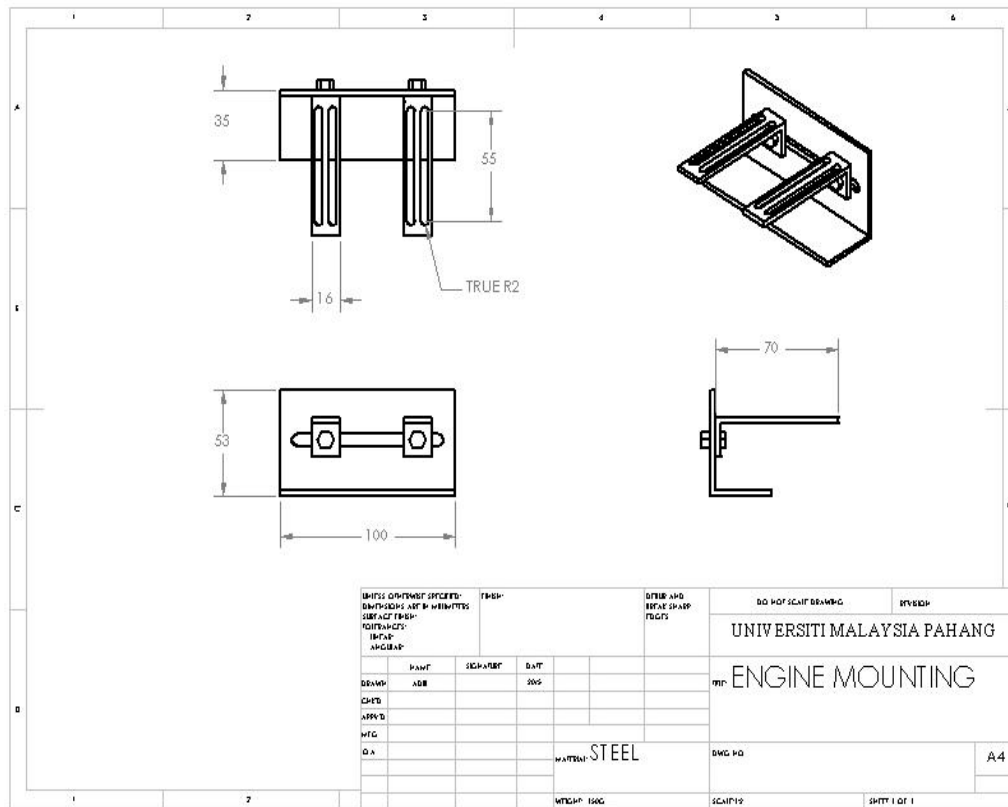


Figure 3.4: The nitro engines mount

3.5.3 Slider

The object that chose as to slide the engine from the base of wood plate is slider from waste of table drawer. It is chosen because it has suitable size and shape to combine another two wood plates that act as slider. Consequently, it also helps to reduce the friction forces that exist from the two wood slides.

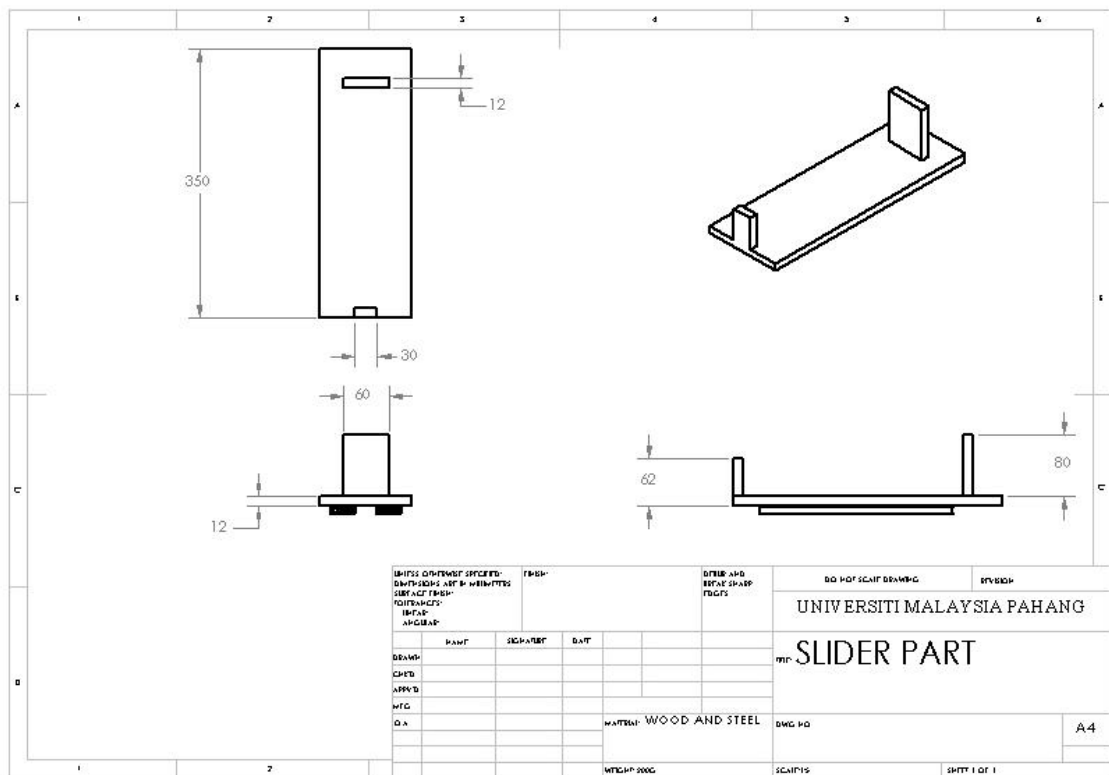


Figure 3.5: The slider part

3.5.4 Nitro Engine

The remote control engine used for this project is Thunder Tiger PRO36 Series. The specifications of the nitro engine are as shown below:

Table 3.1: The Thunder Tiger PRO36 specification

Parameters	Specification
Displacement (c.c)	5.98
Bore (mm)	20.8
Stroke (mm)	17.6
RPM	2000-17000
Output (HP @ rpm)	1.10 @ 16000
Weight (g)	313.6



Figure 3.6: The Thunder Tiger PRO36 series remote control engine

This remote control engine has more cooling fin area to extend the life of the engine and overall tighter needle valve fit utilizes on “O” ring to help maintain the performance levels that needed. The propeller that used is wood type 9×5.

3.5.5 Tachometer

A tachometer is an instrument designed to measure the speed of an object or substance. A tachometer also called as revolution counter is used for measuring rotational speed. It can be used to measure speed of a rotating shaft. Tachometers on aircraft and other vehicles show the rate of rotating of the engine's crankshaft and typically have marking indicating a safe range of rotating speeds. The tachometer is used to measure the needed revolution per minute for experiment setup.



Figure 3.7: The tachometer

3.5.6 Anemometer

Anemometer is used to measure air speed or velocity and airflow volume. Anemometer is a common weather station instrument. The anemometer is used to measure the speed of air in front and rear of the rotating propeller.



Figure 3.8: The anemometer

3.5.7 Spring and Spring Holder

The spring is used to calculate the force exert by the nitro engine.

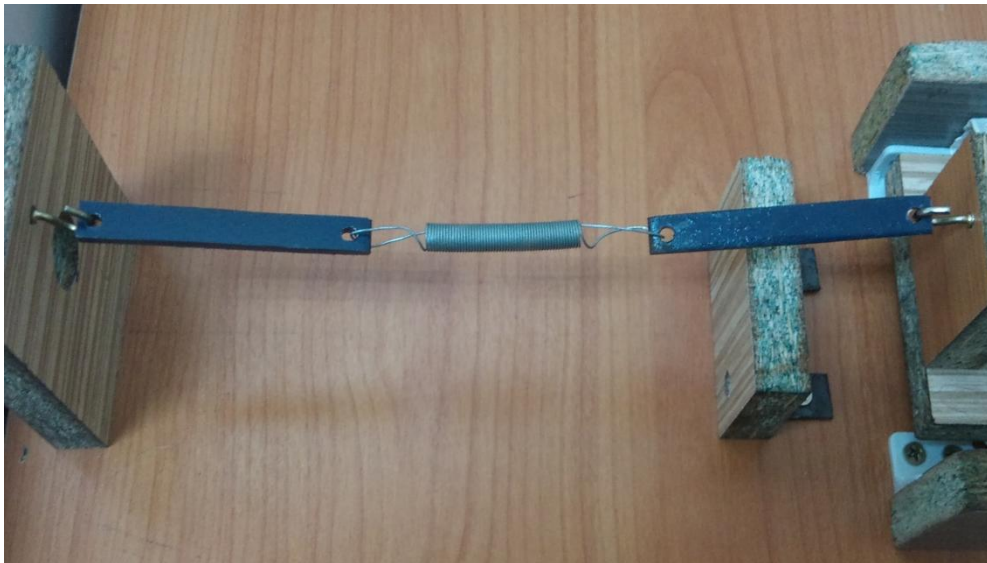


Figure 3.9: The spring

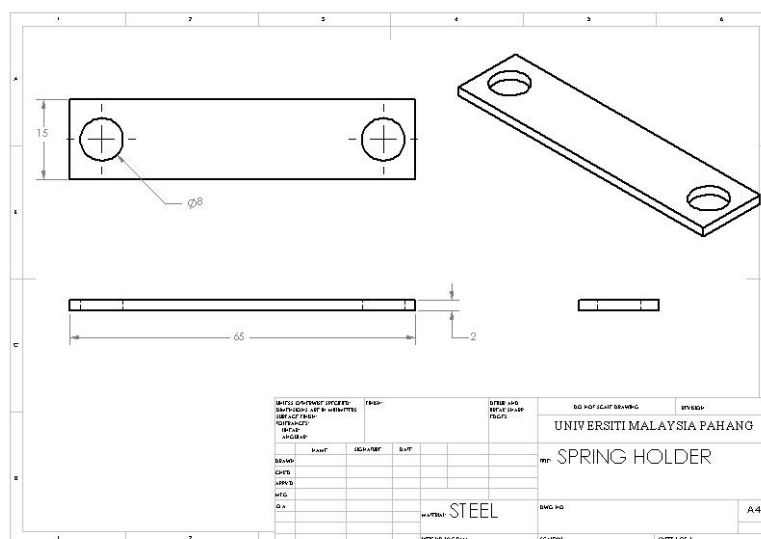


Figure 3.10: The Spring Holder

3.5.8 Oil Tank and Fuel

The oil tank and fuel contain nitro methane is used to power the nitro engine.



Figure 3.11: The oil tank

3.5.9 Servo Set and Electrical Circuit

The servo set and electrical circuit is used to control the speed of nitro engine automatically based on the PIC programming that install in the electrical circuit.

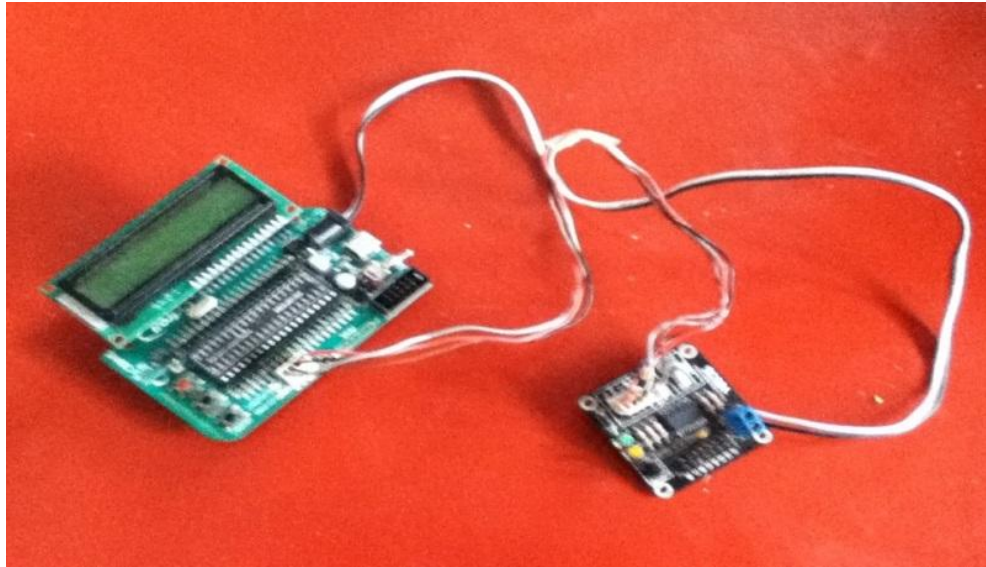


Figure 3.12: The electrical circuit

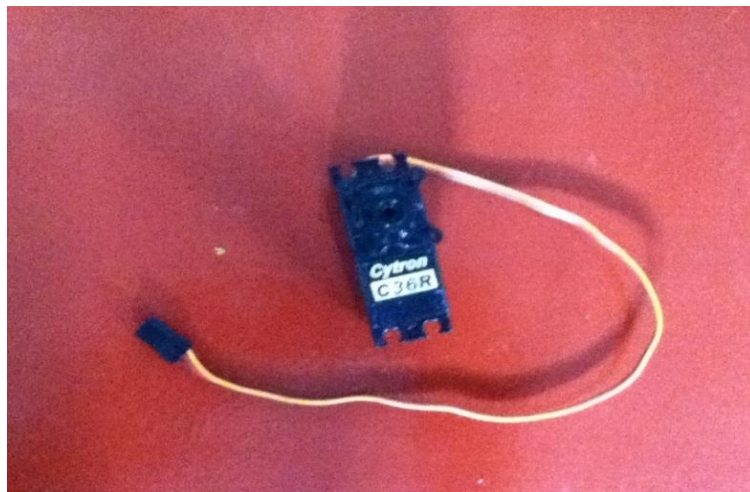


Figure 3.13: The servo

3.6 Fabrication Process

After finalize the design and materials, the next step is fabrication process. The process is making the product based on the design and followed by dimension of the design. Many methods can be used to fabricate a product, like fastening, cutting, drilling and many more. Fabrication process is different from manufacturing process in term of production quantity. Fabrication process is a process to make only one product compared to manufacturing process that focus to large scale production. In the project, fabrication process needed to make the base, engine mounting and slider part. Fabrication process was used at the whole system production. This was included part by part fabrication until assembly the other components.

3.6.1 Processes Involved in Fabrication

In order to make the design come to reality, fabrication process needs to be done first. The fabrication process starts from dimensioning the raw material until it is finished as a desired product. The processes that involved are:

- Measuring: Materials are measured to desired dimensions.
- Marking: All measured materials need to be marked to give precise dimension.
- Cutting: Marked materials are cut into pieces.
- Joining: Materials joined by the method of screw and bolt.
- Drilling: Marked holes are then drilled to make holes for engine mounting slot.
- Finishing: Any uneven and rough surface was flattened by using steel files to give smooth and safe surface.

3.6.2 Steps to Fabricate the Test Bed

After identifying the items that needed to fabricate the test bed, the search process begins. A wooden block from previous projects which is in good condition is reused resulting in reduced cost of fabrication. However, the wooden block has been improved by placing a wooden box made by chipboard to cover the surface of wooden block. There are two slider tracks will be placed on the test bed which are upper slider track and lower slider track. The upper slider track has to be screwed on the base of the

test bed while the lower slider track screwed on the slider. Besides that, the engine mounting needs to be placed on the slider. Next, a holder should be placed at the side of the test bed base so that it is portable to carry the test bed anywhere.

After finishing the parts of the test bed, proceed with the assemble process. Screw two hooks on the slider and the base of the test bed to mount the spring. The engine mounting will be produced in order to fit various sizes and types of engine. The engine mounting will be built using steel plate according to the dimension in the modeling of Design Software.

Build a stand for the oil tank beside the slider and place the oil tank holder on the test bed base. There will be two barriers placed on the oil tank holder to avoid the movement of oil tank during the experiment. The oil tank outlet must be placed equally to the carburetor to ensure the exhaust part produce pressure to allow the nitro flow smoothly. Furthermore, sponge also will be placed on both side of oil tank so that too much of vibration will not be exerted on the oil tank. As a result, air bubble can be avoided in oil tank which may ruin the nitro engine performance.

In addition, servo motor will be placed in servo part which later on placed on the slider part together with the electrical circuit. The purpose of the electrical part and servo motor is to control the engine throttle. Finally, a complete test bed is ready for the experiment.

3.7 EXPERIMENT SETUP

After the engine test bed had been developed for testing process, the nitro engine which is 2-stroke engine can be tested to analysis the performance of engine. Servo motor is programmed to control engine throttle to increase or decrease the engine speed. Therefore, for every 30 seconds the servo which was connected to the throttle will move.

The engine speed will be the control of parameter while the performance parameters will become the variable parameter. The apparatus to measure the value of unknown will be installed to the test bed such as the anemometer to measure the speed rear and front of the propeller, the tachometer to measure the revolution per minute of the propeller, and the LVDT to measure the distance of the spring elongation to get thrust parameter. Hence, the unknown of each mathematical equation will be known by this apparatus. Overall, all of the performance parameters can be obtained by solving the mathematical equations.

3.8 SUMMARY

On the whole, this chapter presents on how the project can be conducted. In fact, while developing the test bed any types of engine could be tested due to the flexibility of the engine mounting design. There are five different speed of engine used in this experiment to obtain results of experiment. Additionally, the value of unknown variables in performance parameters can be obtained by the apparatus and calculated using the mathematical equations as stated in Chapter 2. Hence, the suitable test bed can be suggested according to the types of UVA Propulsion System.

CHAPTER 4

RESULTS AND DISCUSSION

4.1 INTRODUCTION

The purpose of this chapter is to analyze and discuss the results from previous chapter as to be the main outcome of the project. In this chapter, there are some calculation and results of the findings on Thrust, Available Power, Shaft Break Power, Propulsive efficiency, Brake Specific Fuel consumption and Thrust coefficient. According to the results, a graph will be generate and discuss in this chapter. All of the analysis that will be discussed and calculated in this chapter will have to use the formular suggested from the previous chapter.

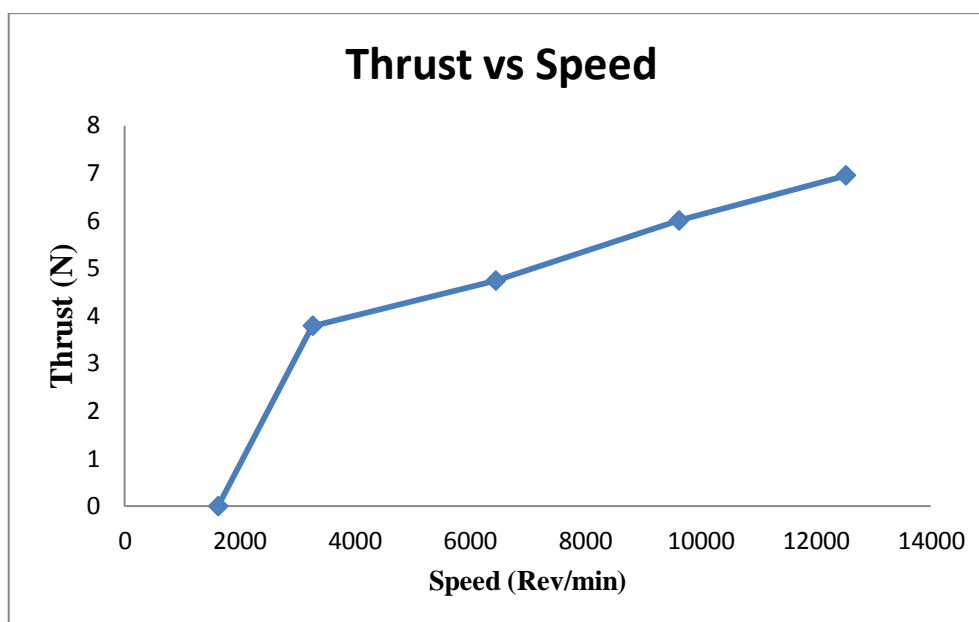
The test bed model is experimented between 1600 to 16000 RPM of nitro engine speed range and the value of performance parameters according to the speed range.

4.2 THRUST

The term thrust, is used to specify the force exert by the engine to slide the slider as mentioned in previous chapter. The force is measured be using the Hooke's Law which is the Thrust (F) is defined as the rate of elongation of the spring (X) times the spring constant (k). Table 4.1 show the force data obtained from the test bed according to five different engines speeds.

Table 4.1: Tabulated data for Thrust.

Engine Speed (RPM)	Elongation of spring, x (m)	Thrust (N)
1618	0.000	0.000
3260	0.012	3.791
6439	0.015	4.739
9621	0.019	6.003
12519	0.022	6.951

**Figure 4.1:** Graph of Thrust vs speed

From the experiment, the thrust was determined at five different speeds, which is 1618 RPM, 3260 RPM, 6439 RPM, 9621 RPM and 12519 RPM by using the slider part that was placed on the base of wood and spring attach to it. The spring constant had been set so that the value of the force can be calculated through the elongation of the spring. The tachometer, was set up in front of the propeller that give the value of the speed propeller and can be set constant while conducting this experiment. According to graph on Figure 4.1, at minimum speed which is 1618 RPM the value of force zero. This is because the speed of propellers is unable to force the slider toward and the spring did not elongated. Assume that the friction force is neglected. Using the equation of Hooke's Law as state above, the value of the force will be zero. The value of force at maximum speed which is 12519 is 7.171N. The graph had shown that the value of force increase by increasing the value of speed. From point 1 to point 2, the gradient is very

high compared to gradient between point 1, point 2, and point 3. As the speed of engine differ, different thrust will be obtain as variable k is always constant and elongation of spring increases according to the engine speeds and hence thrust also increases. Comparing with the previous study, it is proven that graph has nearly the same shape and stiffness but ofcourse the gradient varies as the engine speed obtain are slightly different. The slight different of engine speed is due to random error such as wind speed during the experiment. As stated by Thomad A.ward, the thrust is when the mass flow is not zero through the propeller. The thrust force F_N is dirctely proportional to the mass flow rate, as equation $F_N = \dot{m}(V_e - V_o)$. The engine speed and thrust is zero but when the engine speed increase to 1618RPM the thrust remains zero as shown in graph above. Resulting in the mass flow rate of air through the propeller is in steady state. Steady state means the mass flow rate inlet is equal to the mass flow rate of outlet. Thus, thrust increase when the mass flow is unsteady. The graph shows, the gradient at initial part is very high, due to the slider is on static position and there are no energy to move the slider. Since that, initially to move the slider it needs more energy to move the slider and thats why the gradient of graph at initial part is high.

4.3 AVAILABLE POWER AND SHAFT BRAKE POWER

The available and shaft brake power can be calculated from the test bed. The available power (\dot{W}_A) is define as the rate that useful work is done. The shaft brake power (\dot{W}_B) is define as the power expended by the propeller and imparted to the fluid. Table 4.2 show the available power and shaft brake power data obtained by the test bed according to five different engine speeds.

Table 4.2: Tabulated data for Available Power and Shaft Brake Power.

Engine Speed (RPM)	Velocity inlet, V_o (m/s)	Velocity exit, V_e (m/s)	Available Power, \dot{W}_A (Nm/s)	Shaft Brake Power, \dot{W}_B (Nm/s)
1618	3.43	8.57	0	0
3260	4.70	9.60	17.82	27.12
6439	5.23	10.86	24.78	35.04
9621	5.73	11.73	34.40	40.53
12519	6.43	12.67	44.69	51.79

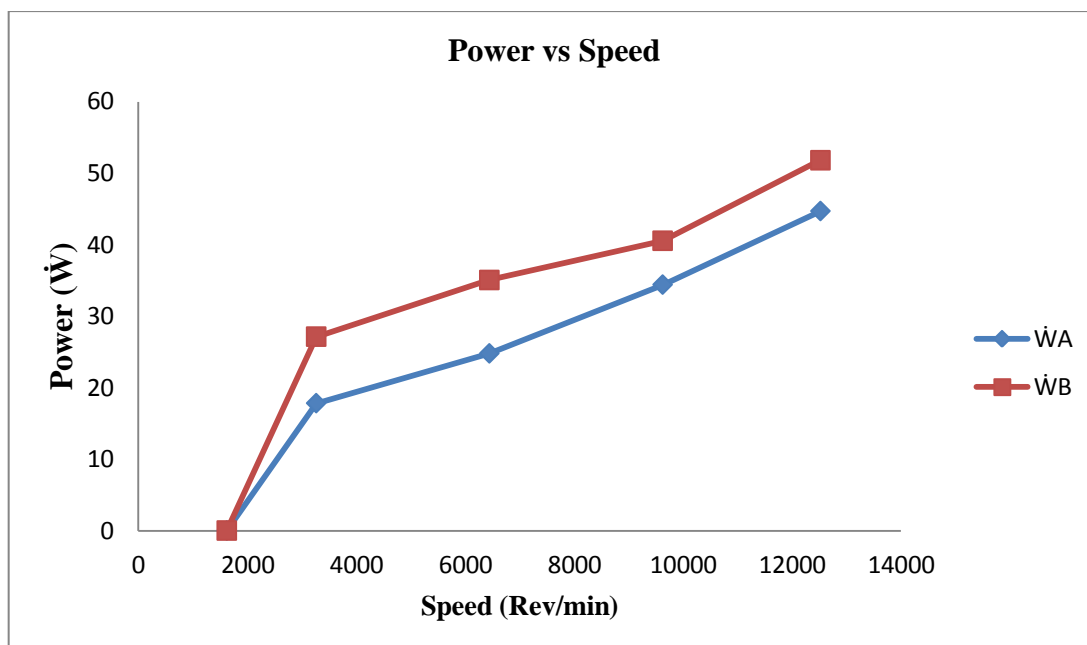


Figure 4.2: Graph of Available and Shaft Brake Power versus Speed.

From the experiment the available power and shaft brake power was determined at five different speeds, which are 1618 RPM, 3260 RPM, 6439 RPM, 9621 RPM, and 12519 RPM by using the anemometer to measure the speed of the air inlet and exit from propeller. The anemometer was set up in front and rear of the propeller, this anemometer will give the value of the air speed so that both powers can be calculated by using the exact equation as show above. According to the graph on Figure 4.2, at minimum speed which is 1618 RPM the values of both powers are zero. It is because the force as discussed above is zero and assume that friction force is neglected. The value of available power at maximum speed which is 12519 RPM is 51.96 Nm/s meanwhile the value of brake shaft power at the same speed is 76.69 Nm/s. The graph shows that the value of both powers increase by the increasing value of speed. This values can be obtain by deriving the basic law of Isaac Newton which is $F=ma$. After deriving from the previous formular, $W_A=F_N V_o$ is formed and the result of the conducted experiment can be obtained. The graph above clearly shows that, power of engine directly proportional to engine speed. The result obtained from this experiment is approximately same with previous study. Hence, it can be concluded that the power of engine increases with the increasing speed engine. Slight difference of values are due to random errors such as wind. From the graph, the brake shaft power is greater than

available power. The shaft brake power is equal to the power expended by the propeller and imparted to the fluid. The available power is the rate that useful work is done. Shaft brake power expressed in Imperial units of horsepower is referred to shaft horsepower. Brake horsepower is slightly different because it is a measure of engine's horsepower without losses due to the gearbox or auxiliary components. The shaft brake power cannot be perfectly transmitted to the propeller as available power in the actual piston aero engines due to losses associated with the compressibility of air, as stated by Thomas A. Ward in *Aerospace Propulsion Systems*. This results in the available power less than the shaft power.

4.4 PROPULSIVE EFFICIENCY

The propulsive efficiency (η_p) is defined as the fraction of shaft brake power delivered to the propeller and converted into propeller thrust power (Available Power). The propeller efficiency (η_{prop}) is generally equal to the propulsive efficiency (η_p) for aero piston engines. Table 4.3 shows the propulsive efficiency data obtained by the test bed according to five different engine speeds.

Table 4.3: Tabulated data for Propulsive Efficiency

Engine Speed (RPM)	Available Power, \dot{W}_A (Nm/s)	Shaft Brake Power, \dot{W}_B (Nm/s)	Propulsive Efficiency, η_p (%)
1618	0	0	0.000
3260	17.82	27.12	65.70
6439	24.78	35.04	70.72
9621	34.40	40.53	84.88
12519	44.69	51.79	86.31

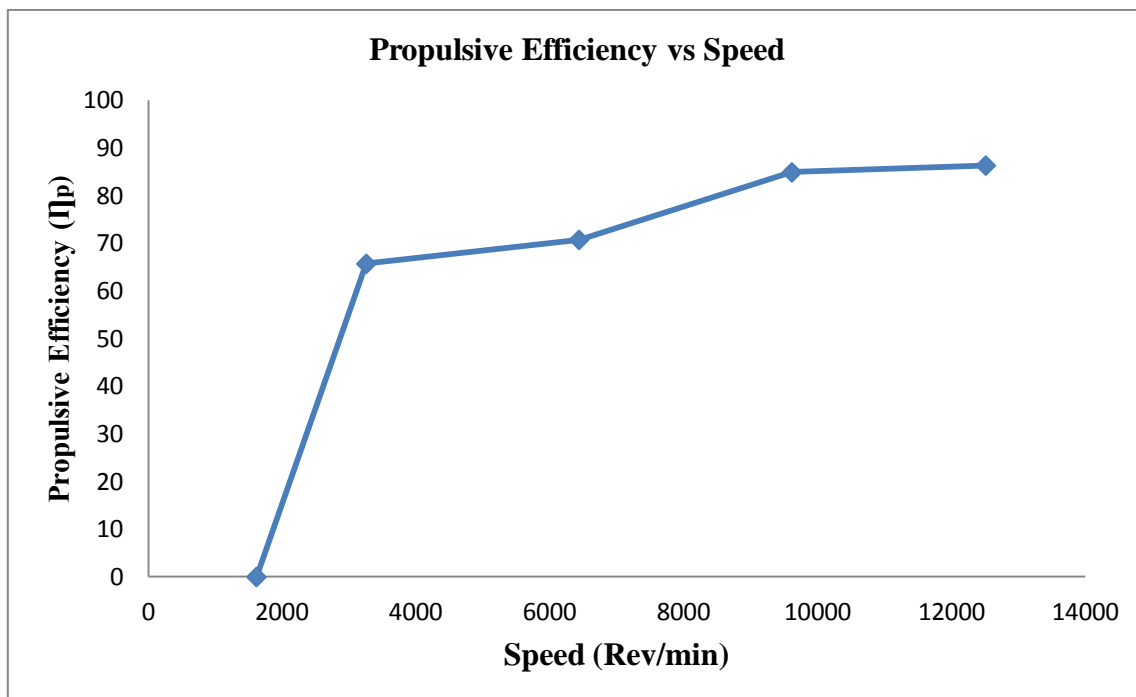


Figure 4.3: Graph of Propulsive Efficiency versus Speed

From the experiment, propulsive efficiency was determined at five different speeds, which is 1618 RPM, 3260 RPM, 6439 RPM, 9621 RPM, and 12519 RPM by using the anemometer to measure the speeds of the air inlet and exit from propeller. The value of the propulsive efficiency can be calculated by divided the value of available power to the shaft brake power. According to the graph on Figure 4.3, at minimum speed which is 1618 RPM the value of propulsive efficiency is zero. This is because both powers described previously cannot be calculated due to the spring that is not elongate at minimum speed as discussed above and friction force was assumed to be neglected. The value of propulsive efficiency at 3260 RPM is 65.70% meanwhile the value of propulsive efficiency at maximum speed which is 12519 RPM is 86.31%. The graph had shown that the value of propulsive efficiency increase by the increasing value of speed. The graph above shows an increasing gradient and it is approximately same with the previous study. However, the shape of this graph is not a constant straight line due to minor errors such as random error caused by wind flow during experiment. Very high propulsion efficiencies are achievable for low and medium subsonic speed ranges. This happens when the propeller achieves a specified amount of trust by giving a relatively small acceleration correspondingly to large volume of air, as stated by Thomas A.Ward in Aerospace Propulsion Systems.

4.5 BRAKE SPECIFIC FUEL CONSUMPTION

The brake specific fuel consumption (BSFC) is defined as the rate of fuel consumption or mass flow rate of fuel (\dot{m}_{fuel}) divided by the rate of shaft brake power (\dot{W}_B) production. From the definition of BSFC it is clear that lower values represent more fuel efficient engines. Table 4.4 show the BSFC data obtained by the test bed according to five different engine speeds.

Table 4.4: Tabulated data for Brake Specific Fuel Consumption.

Engine Speed (RPM)	Mass of fuel m, (kg)	Mass flow rate of fuel, \dot{m}_{fuel} (kg/sec)	Brake Specific Fuel Consumption, BSFC ($\mu\text{g}/(\text{W}\cdot\text{s})$)
1618	0.0063	2.100×10^{-5}	/
3260	0.0153	5.100×10^{-5}	1.8805
6439	0.0246	8.200×10^{-5}	2.3402
9621	0.0357	1.190×10^{-4}	2.9361
12519	0.0487	1.623×10^{-4}	3.1356

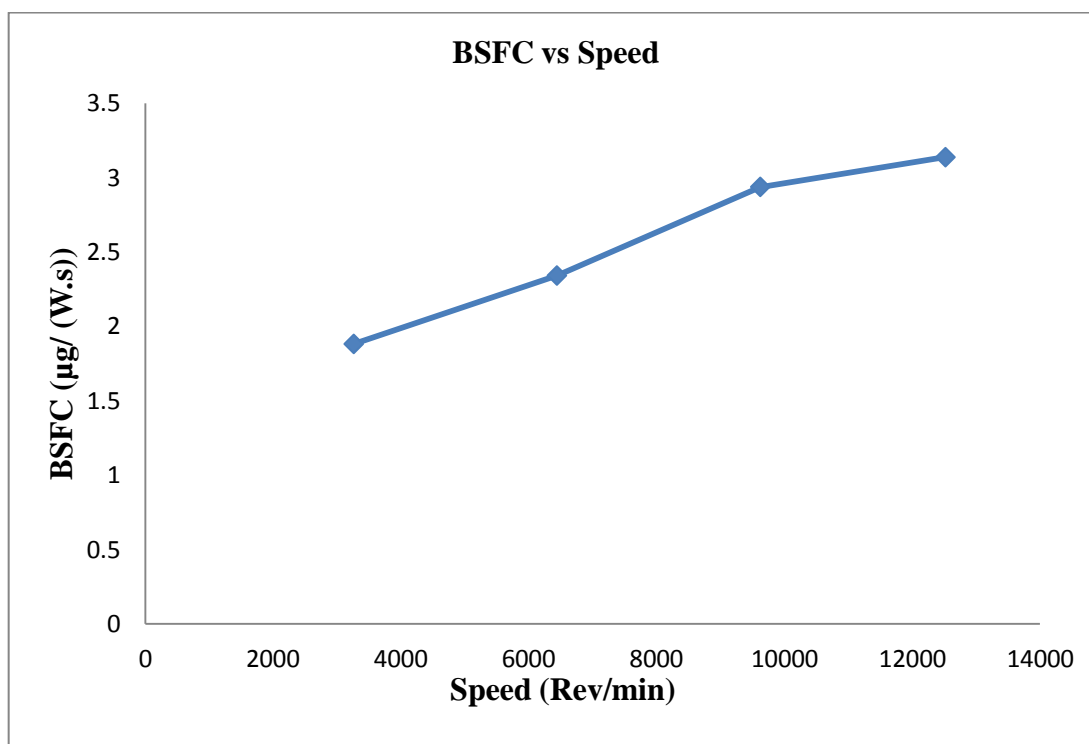


Figure 4.4: Graph of Brake Specific Fuel Consumption versus Speed

From the experiment the BSFC was determined at five different speeds, which are 1618 RPM, 3260 RPM, 6439 RPM, 9621 RPM, and 12519 RPM by using the oil tank with a level to measure the fuel usage while the nitro engine operates at different speeds. Five minutes are given to the nitro engine to run at different speeds while times are taken by using a stopwatch. The value of the BSFC can be calculated by calculating the mass flow rate of fuel (\dot{m}_{fuel}) first before dividing it by the shaft brake power (\dot{W}_B) as shown above. According to the graph on Figure 4.4, at the minimum speed which is 1618.62 RPM the value of BSFC cannot be calculated. It is because the shaft brake power cannot be determined. The value of BSFC at 3260 RPM is 1.8805 $\mu\text{g}/(\text{W}\cdot\text{s})$ meanwhile the value of propulsive efficiency at maximum speed which is 12519 RPM is 3.1356 $\mu\text{g}/(\text{W}\cdot\text{s})$. The graph had shown that the value of BSFC increases by the increasing of the value of speed. BSFC is directly proportional to engine volume, such as engine volume goes down so does BSFC. This is due to the heat losses from the end gas to the cylinder walls. Higher engine speeds produce a high BSFC because of rising friction losses in the engine. Higher friction losses reduce brake torque, which increases BSFC. This increase can be explained by using Isaac Newton's Third Law, every action has an equal reaction. As the engine speed increases there is a direct flow of wind from the opposite direction that causes friction between the wind formed by the engine and wind from the environment causing a slight decrease of engine power and this is the cause of an increase in BSFC of the engine. The richer mixture ratio used will make the BSFC increase because the fuel mass flow increases as the shaft brake power is reduced. At idle the BSFC is high, because the closed throttle causes pumping losses and excessive camshaft overlap. Minimum BSFC occurs at a shaft speed that gives the peak torque operating point. This is the most fuel-efficient operating point for an engine. When the shaft speed continues to increase, the BSFC also increases since more fuel is required to overcome speed-induced friction and air intake mass flow limitations. Higher compression engines generally have a lower BSFC than lower compression engines. The engines that use carburetors will have a slightly greater BSFC than direct injection engines. Addition of a supercharger increases the BSFC at low shaft speeds as stated by Thomas A. Ward in *Aerospace Propulsion Systems*.

4.6 THRUST COEFFICIENT

The Thrust Coefficient (C_f) is defined as the Thrust (F_N) divided by fluid density, ρ , revolution per second, n_{prop} and diameter of circular disk formed by rotating propellers, d production. Table 4.5 show the Thrust Coefficient data obtained by the test bed according to five different engine speeds.

Table 4.5: Tabulated data for Thrust Coefficient (C_f).

Engine Speed (RPM)	Engine Speed (RPS)	Thrust (F_N, N)	Thrust Coefficient (C_f)
1618	26.9770	0.000	0
3260	54.3415	3.791	0.3745
6439	107.3287	4.739	0.1200
9621	160.3543	6.003	0.0681
12519	208.6600	6.951	0.0466

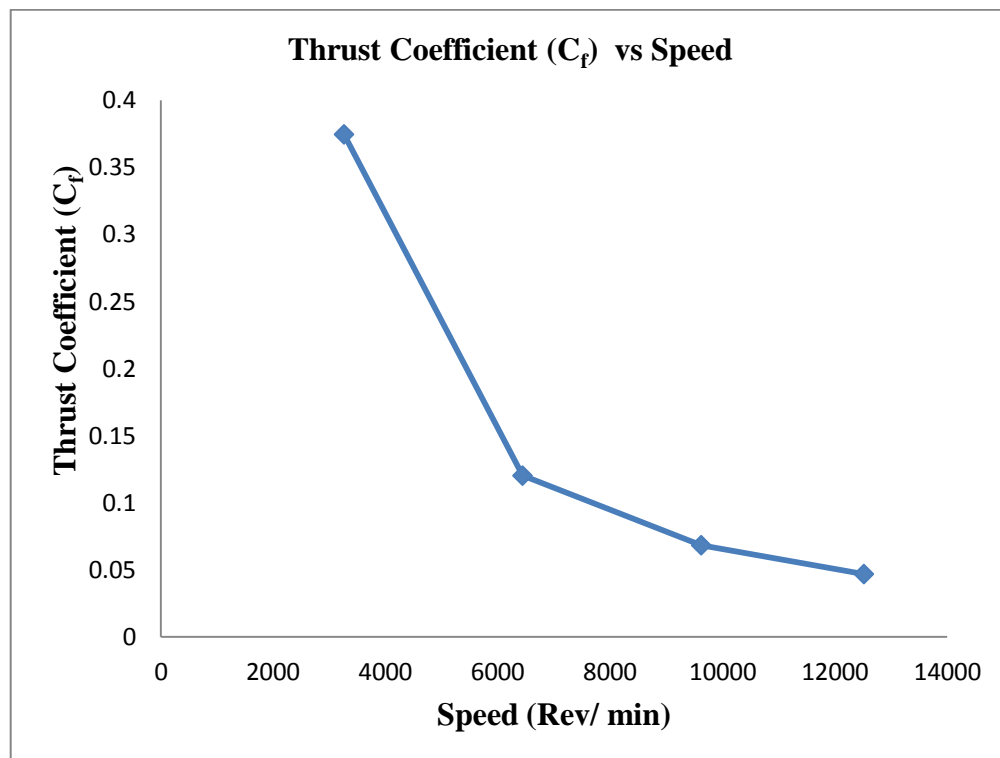


Figure 4.5: Graph of Thrust Coefficient (C_f) versus Speed

From the experiment the Thrust Coefficient was determined at five different speeds, which are 1618 RPM, 3260 RPM, 6439 RPM, 9621 RPM, and 12519 RPM by using the formula while the nitro engine is operating at different speeds. The value of the Thrust Coefficient can be calculated by Thrust (F_N) divided by fluid density, ρ , revolution per second, n_{prop} and diameter of circular disk formed by rotating propellers, d production as shown above. According to the graph on Figure 4.5, at minimum speed which is 1618 RPM the value of Thrust Coefficient is Zero. It is because the Thrust is Zero. The value of Thrust Coefficient at 3260 RPM is 0.3745 meanwhile the value of Thrust Coefficient at maximum speed which is 12519 RPM is 0.0466.

4.7 SUMMARY

From this experiment, the result shows that the performance parameters increase along the increasing of speed. The obtained data from performance parameters are proportional to the speed. The data from the nitro engine can be obtained and analyzed by designing and fabricating the test bed without using the actual body of remote control aircraft. The test bed is able to perform detail testing at various RPM settings and nitro engines. All the performance parameters needed can be calculated from this test bed by using the apparatus such as tachometer and anemometer that has been set up along the process of designing and this will reduce the time and cost to test the nitro engine by using the actual body of aircraft.

CHAPTER 5

CONCLUSIONS AND RECOMMENDATIONS

5.1 CONCLUSIONS

A test bed model had been produced based on the project title which is to design, analysis and performance testing of UAV propulsion system. The detail design of test bed model had been modeled by using the Design Software to produce the actual body of test bed model.

The test bed design model has been designed for experimenatation with intergreted with PIC microcontroller. The PIC microcontroller able to control the engine trottle. The test bed design is very comperhensive and can measureble five differences performance parameters.

The performance parameters such as thrust, available power, shaft brake power, propulsive efficiency, brake specific fuel comsumption and thrust coeffient can be calculated by using the test bed. The apparatus such as anemometer and tachometer that had been setup are used to find unknown variables that exit in any equation involve in this project.

The variables that is setup in this project is the speed of the nitro engine. The five different speeds had been setup to study and analysis the connection between the variable and the performance parameters. All the objectives which is to design a comprehensive test bed for detail testing, to analyze the designed test bed for data collection reliability to the test bed, and to perform detail testing for nitro engine at various RPM setting and evaluate corresponding performance parameter associated to the setting were achieved.

From this project, the detail design of test bed model had been modeled by using the Design Software to produce the actual body of test bed model. Fabricate the product by using any kind of facility that were exists in laboratory such as cutting the material using grinder and hand saw, join all parts with set of screw, bending the sheet metal by using bending machine. Moreover, this project also include the PIC microcontroller to control engine throttle.

5.2 RECOMMENDATIONS

In near future, there are several recommendation for further studies as below:

1. The further study can be made with more parameters, various sizes and ratings engine, different types and sizes of propeller. The data that will be obtained can be used to compare to this data on this study. Parameters that can recommend are air ratio, induced power, induced efficiency and power coefficient.
2. When the engine at full throttle, vibration of the engines is so huge. Due to this problem, the bolts and nuts will be baggy. For the recommendation, the further test bed must reduce the vibration of engine to avoid undesirable incidents.
3. Weight of the test bed is too heavy and difficult to carry to anywhere. Even when the holder is provide, this method cannot reduce the problem. However, this problem can be overcome by changing the material for base of the test bed with a box of chipboard.

REFERENCES

- ASTM. (2005). *Standard terminology for unmanned air vehicle systems*. F2395-05.
ASTM International: West Conshohocken, PA.
- Bird, B. (2005). *Model airplane secrets, basic to advanced strategies on model building*.
- Fahlstrom, P.G. & Gleason, T.J. (1998). *Introduction to UAV Systems*. Columbia, MD: UAV Systems, Inc.
- Herwitz, S.R., Johnson, L.F., Dunagan, S.E., Higgins, R.G., Sullivan, D.V., Zheng, J., Lobitz, B.M., Leung, J.G., Gallmeyer, B.A., Aoyagi, M., Slye, R.E., & Brass, J. (2004). Demonstration of UAV-based imaging for agricultural surveillance and decision support.
- Herwitz, S.R., Dolci, R.J., Berthold, R.W. & Tiffany, G.C. (2005). Chemical sensing from a low-flying UAV: data for first responders during a staged terrorist event. *Proceedings of Department of Homeland Security Partnering Conference*: Boston, MA.
- Hobbico, I. (2000). *Owner's Instruction Manual*. O.S. Engines Mfg. Co., Ltd.
- Newcome, L. R. (2004). *Unmanned Aviation: A brief history of unmanned aerial vehicles*. AIAA: Reston, VA.
- Anderson, J.D. 1999. *Aircraft Performance and Design*. Singapore: Mc Graw Hill.
- Avalakki, N., Bannister, J., Chartier, B., Downie, T., Gibson, B., Gottwald, C., Moncrieff, P. and Williams, M. 2007. Design, Development and Manufacture of a Search and Rescue Unmanned Aerial Vehicle. University of Adelaide, Australia.
- Cengel, Y.A., Cimbala, J.M. 2006. *Fluid Mechanics, Fundamental and Applications*. Singapore: Mc Graw Hill.
- Office of Secretary of Defense. (2002). *Unmanned Aerial Vehicles Roadmap*. Washington, DC: Author.

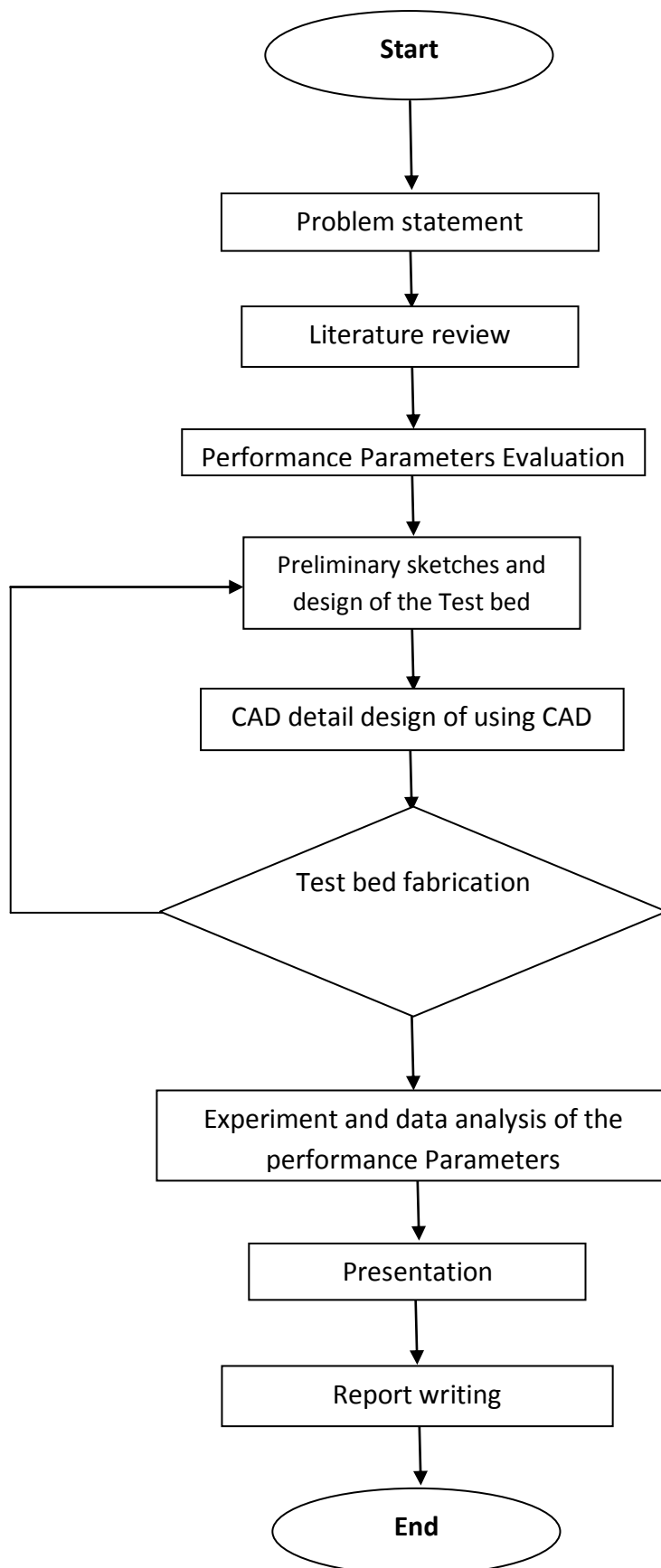
- Raine, R.R., Moyle, K., Gordon and Robertson, J., (2002). *A Cost-Effective Teaching and Research Dynamometer for Small Engines*.
- Tressler, R. (2008). *Getting started with radio controlled model airplanes, a beginner's tutorial*.
- Ward, T.A. (1966). *Aerospace Propulsion Systems*. John Wiley and Sons (Asia). Singapore.

APPENDICE A1

GANTT CHART FOR FYP 1

Project Progress	Week 1	Week 2	Week 3	Week 4	Week 5	Week 6	Week 7	Week 8	Week 9	Week 10	Week 11	Week 12	Week 13	Week 14
1. Get the project title														
2. Search the information of project														
3. Overview of the project														
4. Finding Literature Review														
5. Parameters Analysis														
6. Preliminary Sketches and Design														
7. CAD detail design of using CAD														
8. Programming for rpm controller														
9. Cooling System														
10. Final Draft Fyp 1 Submission														
11. Presentation														

APPENDICE A3
FLOW CHART OF OVERALL FYP



APPENDICE A3
The Raw Data from The Experiment

Engine Speed (RPM)	Elongation of Spring (m)	Velocity inlet (m/s)	Velocity outlet (m/s)	Mass (kg)	Thrust (N)	Available power (Nm/s)	Shaft Brake power (Nm/s)	Propeller Efficiency	BSFC ($\mu\text{g}/(\text{W}\cdot\text{s})$)
1618.62	0.000	3.43	8.57	0.0063	0.000	0	0	0.000	/
3260.49	0.012	4.70	9.60	0.0153	3.791	17.82	27.12	65.70	1.8805
6439.26	0.015	5.23	10.86	0.0246	4.739	24.78	35.04	70.72	2.3402
9621.26	0.019	5.73	11.73	0.0357	6.003	34.40	40.53	84.88	2.9361
12519.60	0.022	6.43	12.67	0.0487	6.951	44.69	51.79	86.31	3.1356

APPENDICE A4
CALUATION OF THRUST

Tabulated data for Thrust.

Engine Speed (RPM)	Elongation of spring, x (m)	Thrust (N)
1618.62	0.000	0.000
3260.49	0.012	3.791
6439.26	0.015	4.739
9621.26	0.019	6.003
12519.60	0.022	6.951

Example calculation of force:

By using the Hooke's Law equation as state in Chapter 2 as Eq. (2.2). The spring constant, k= 315.94 N/m.

At maximum engine speed = 12519.60 RPM

The elongation of spring, x=0.0223m

Hence, $F = Kx$

$$= (315.94 \text{ N/m})(0.022)$$

$$= 6.951 \text{ N}$$

APPENDICE A5

CALUATION OF AVAILABLE POWER AND SHAFT BREAK POWER

Examples of calculation of Available Power:

The available power is the rate that useful work is done, as state in Chapter 2 as Eq. (2.3),

At maximum engine speed = 12519.60 RPM

The velocity if air inlet through the propeller, $V_o = 6.43$ m/s

$$\begin{aligned} \text{Hence, } \dot{W}_A &= F_N V_o \\ &= (6.951 \text{ N})(6.43 \text{ m/s}) \\ &= 44.69 \text{ N m/s} \end{aligned}$$

Example of calculation of Shaft Brake Power:

The shaft brake power is simply the rate of change in kinetic energy of the flow passing through it, as state in Chapter 2 as Eq.(2.4).

$$\dot{m} = 0.869 \text{ N.ms}^{-2}$$

At maximum speed engine = 12519.60 RPM

The velocity of air inlet, $V_o = 6.43$ m/s

The velocity of air exit, $V_e = 12.67$ m/s

$$\begin{aligned} \text{Hence, } \dot{W}_B &= \dot{m} \left[\left(\frac{V_e^2}{2} \right) - \left(\frac{V_o^2}{2} \right) \right] \\ &= 0.869 \text{ N.ms}^{-2} \left[\left(\frac{12.67^2}{2} \right) - \left(\frac{6.43^2}{2} \right) \right] \\ &= 51.79 \text{ Nm/s} \end{aligned}$$

APPENDICE A6
CALUATION OF PROPULSIVE EFFICIENCY

Engine Speed (RPM)	Available Power, \dot{W}_A (Nm/s)	Shaft Brake Power, \dot{W}_B (Nm/s)	Propulsive Efficiency, η_p (%)
1618.62	0	0	0.000
3260.49	17.82	27.12	65.70
6439.26	24.78	35.04	70.72
9621.26	34.40	40.53	84.88
12519.60	44.69	51.79	86.31

Example of calculation of propulsive efficiency:

The propulsive efficiency relates the fraction of shaft brake power delivered to the propeller and converted into propeller thrust power (available power), as state in Chapter 2 as Eq. (2.5).

At maximum engine speed = 12519.60RPM

The available power = 44.69 Nm/s

The shaft brake power = 51.79Nm/s

Hence,

$$\eta_p = \frac{\dot{W}_A}{\dot{W}_B}$$

$$= \frac{44.69}{51.79}$$

$$= 0.86 \approx 86.31\%$$

APPENDICE A7
CALUATION OF BRAKE SPECIFIC FUEL CONSUMPTION

Engine Speed (RPM)	Mass of fuel m, (kg)	Mass flow rate of fuel, \dot{m}_{fuel} (kg/sec)	Brake Specific Fuel Consumption, BSFC ($\mu\text{g}/(\text{W.s})$)
1618.62	0.0063	2.100×10^{-5}	/
3260.49	0.0153	5.100×10^{-5}	1.8805
6439.72	0.0246	8.200×10^{-5}	2.3402
9621.26	0.0357	1.190×10^{-4}	2.9361
12519.60	0.0487	1.623×10^{-4}	3.1356

Example of calculation of specific fuel consumption:

The equation of specific fuel consumption is simply the mass flow rate of fuel (\dot{m}_{fuel}) divided by the rate of shaft brake power (\dot{W}_B) production, as state in Chapter 2 as Eq. (2.6).

At maximum engine speed = 12519.60 RPM

The mass of fuel used = 0.0487 kg

The engine runs for 5 minute = 300 sec

$$\dot{m}_{fuel} = \frac{\text{mass}}{\text{Time}}$$

$$\dot{m}_{fuel} = \frac{0.487\text{kg}}{300\text{s}}$$

$$= 1.623 \times 10^{-4} \text{ kg/sec}$$

Hence,
$$\text{BSFC} = \frac{\dot{m}_{fuel}}{\dot{W}_B} = \eta_p \frac{\dot{m}_{fuel}}{\dot{W}_A}$$

$$\text{BSFC} = \frac{1.623 \times 10^{-4}}{51.79}$$

$$= 3.1356 \mu\text{g}/(\text{W.s})$$

APPENDICE A7
CALUATION OF THRUST COEFFICIENT

Engine Speed (RPM)	Engine Speed (RPS)	Thrust (F_N,N)	Thrust Coefficient (C_f)
1618.62	26.9770	0.000	0
3260.49	54.3415	3.791	0.3745
6439.72	107.3287	4.739	0.1200
9621.26	160.3543	6.003	0.0681
12519.60	208.6600	6.951	0.0466

Example of calculation of Thrust Coefficient (C_f):

The equation of Thrust Coefficient (C_f) is simply the the Thrust (F_N) divided by fluid density, ρ, revolution per second, \mathbf{n}_{prop} and diameter of circular disk formed by rotating propellers, d production, as state in Chapter 2 as Eq. (2.7).

At maximum engine speed = 12519.60 RPM

At maximu engine speed (RPS) = 208.6600 RPS

Desity of air, ρ = 1.225 kg/m³

Diameter of blades: 22.83cm = 0.23m

Hence,

$$\begin{aligned}
 C_f &= \frac{F_N}{\rho \mathbf{n}_{prop}^2 d^4} \\
 &= \frac{6.951}{(1.225) 208.66^2 (0.23)^4} \\
 &= 0.0466
 \end{aligned}$$

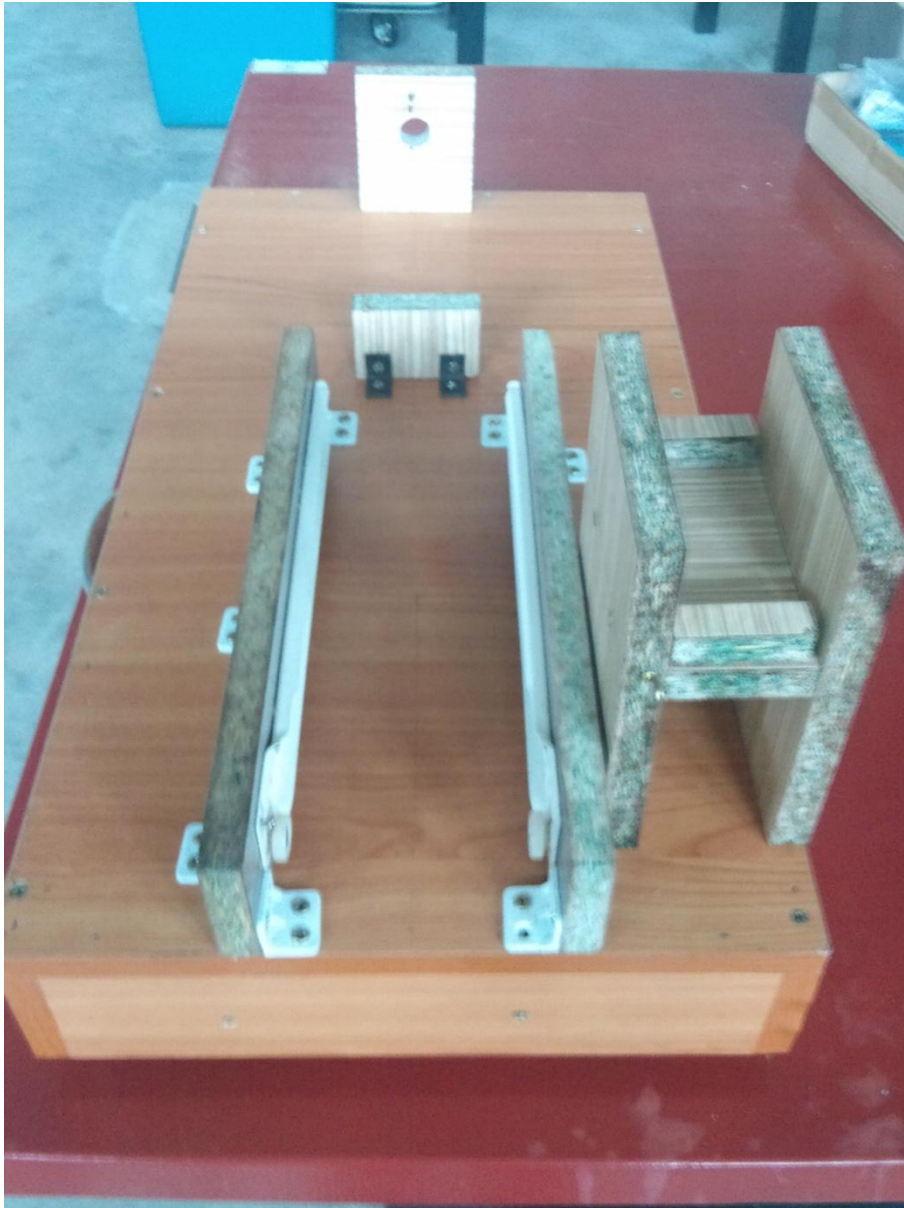
APPENDICE B1
ACTUAL TEST BED DESIGN



APPENDICE B2
The Engine and Propeller
(Thunder Tiger PRO36)



APPENDICE B3
The Base Of Test Bed

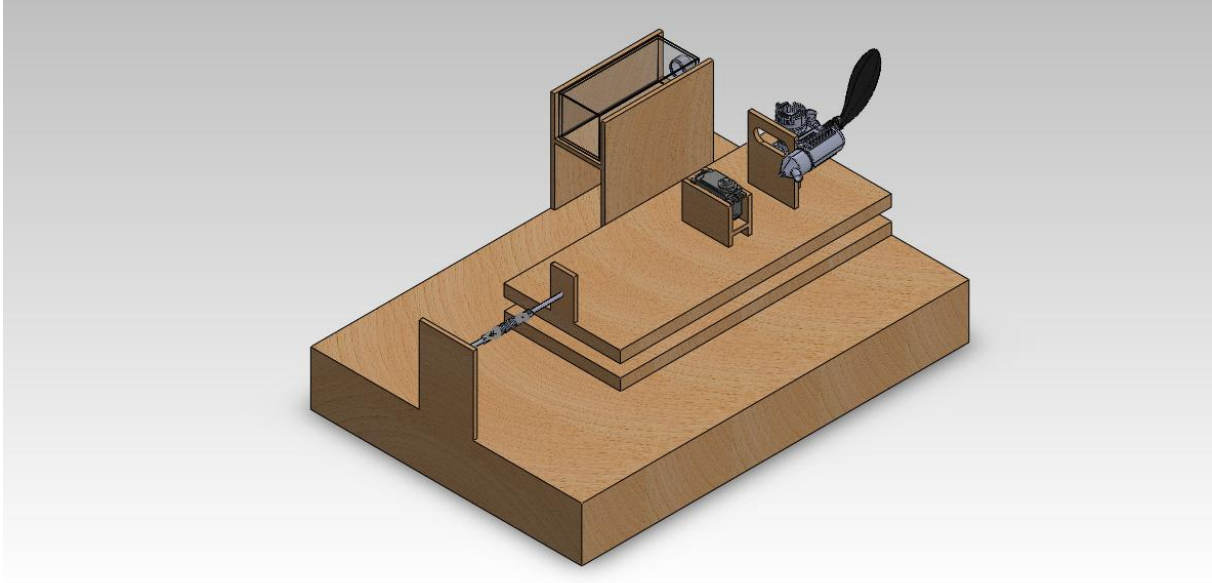


APPENDICE B4

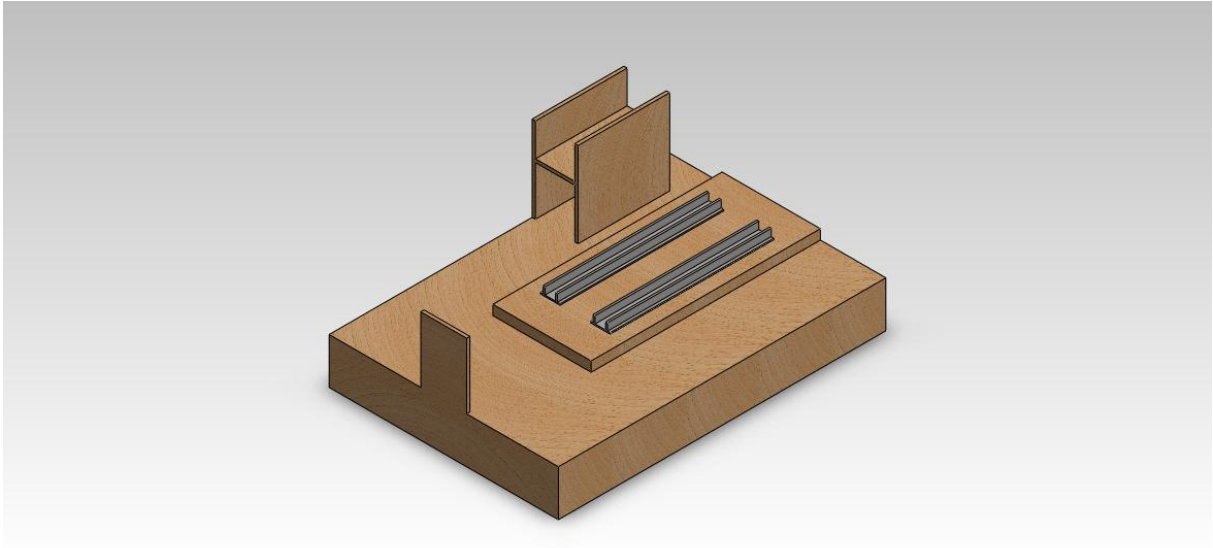
The PIC Microcontroller



APPENDICE C1
The Design Of Base Of Test Bed in Solidworks



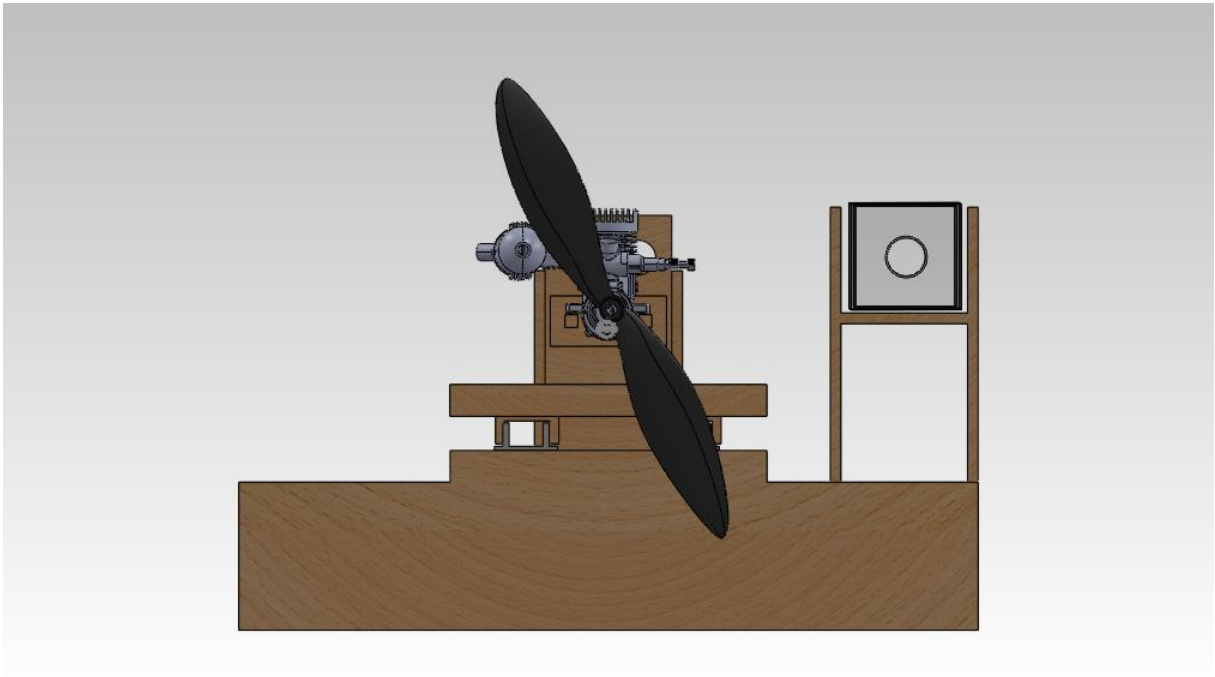
APPENDICE C2
The Design Of The Base of Test bed



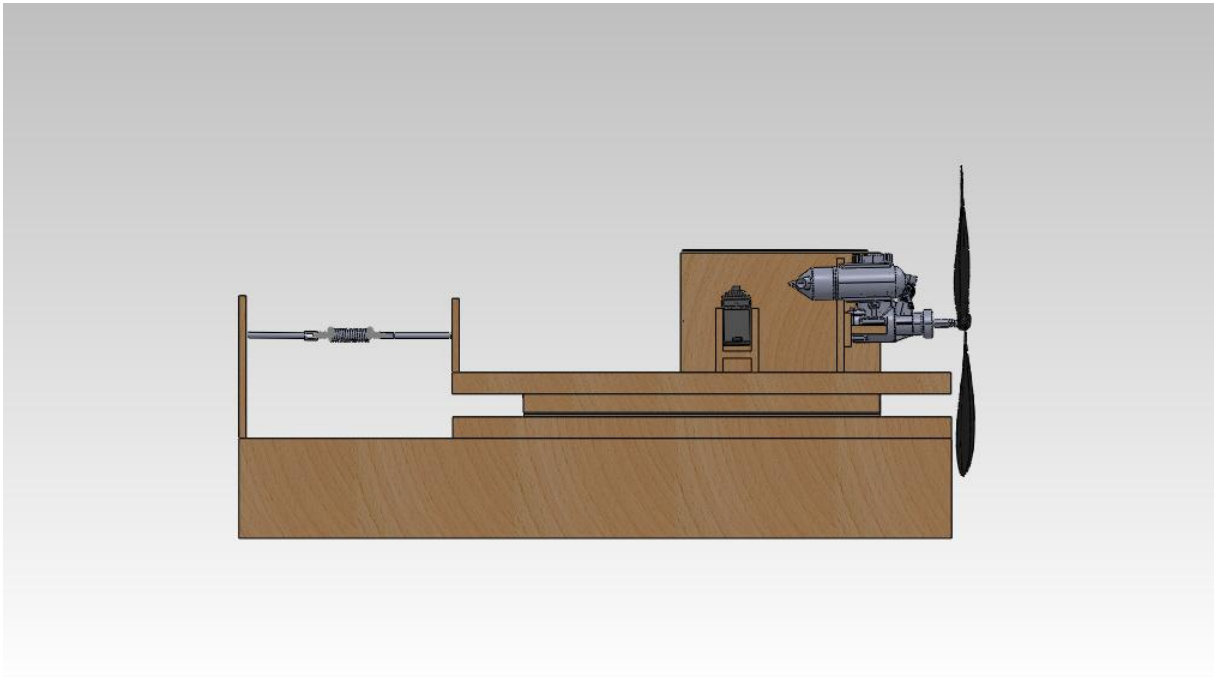
APPENDICE C3
The Top View Of The Test Bed



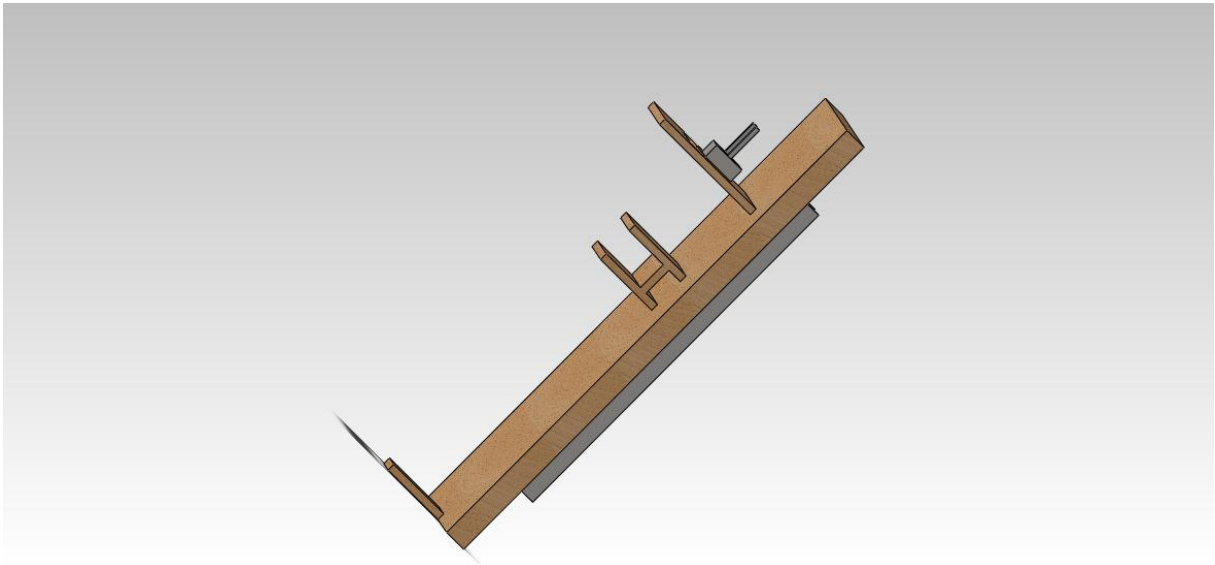
APPENDICE C4
The Front View Of The Test Bed



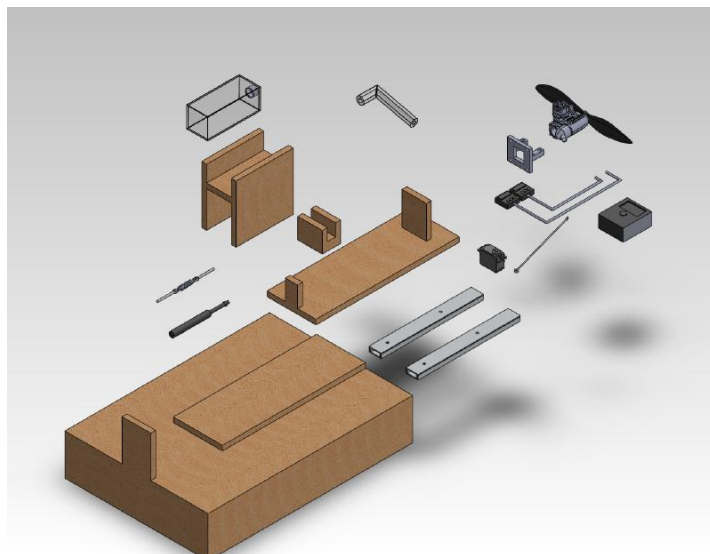
APPENDICE C5
The Side View Of The Test Bed



APPENDICE C6
The Slider Part Of The Test Bed

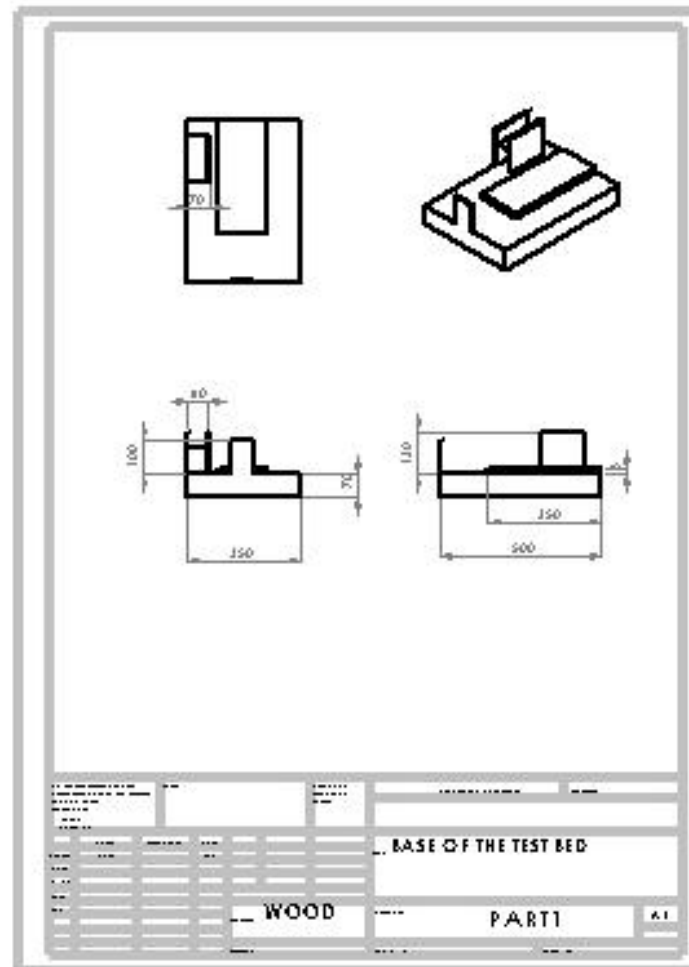


APPENDICE C7
The Exploded Drawing Of The Test Bed



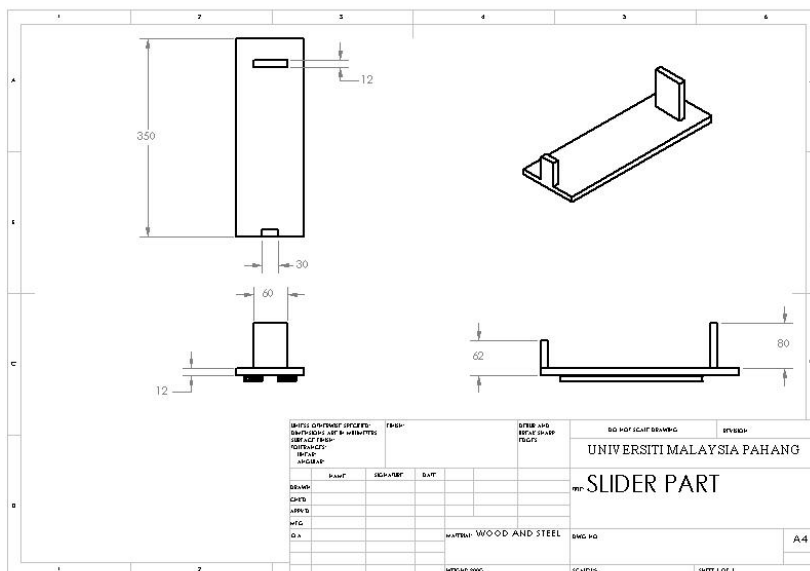
APPENDICE D1

The Orthographic Drawing Of The Test Bed's Base



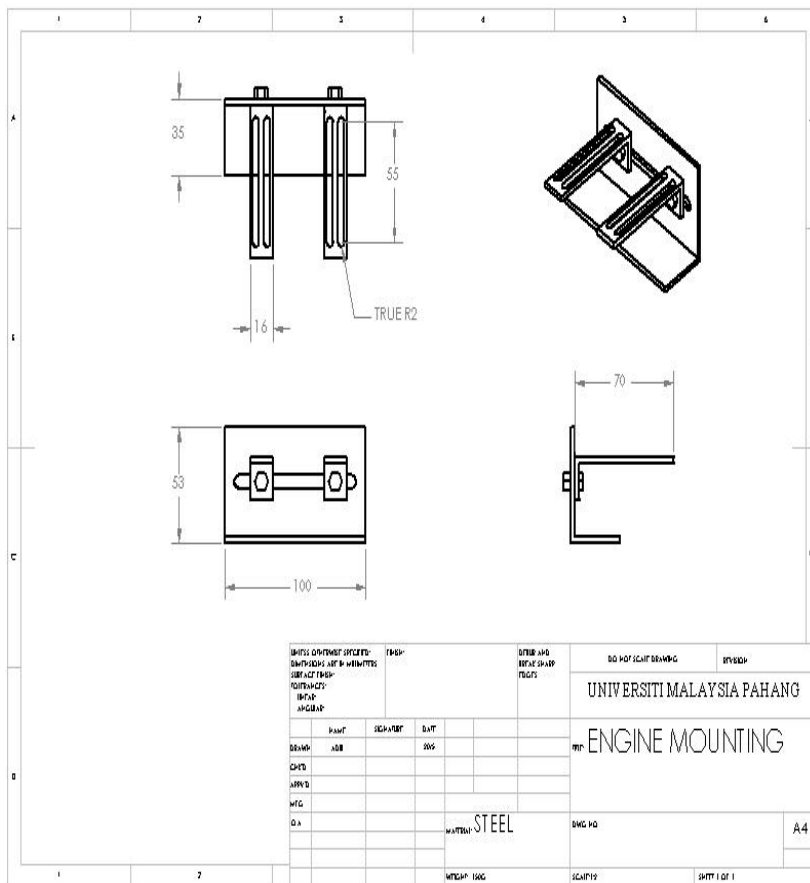
APPENDICE D2

The Orthographic Drawing Of Slider Part



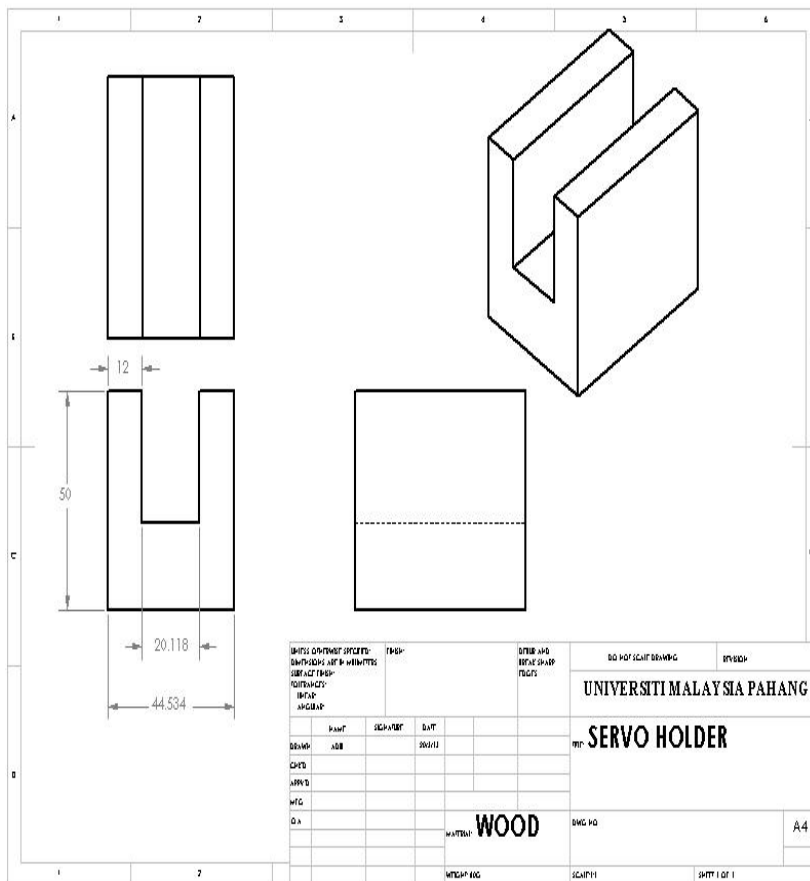
APPENDICE D4

The Orthographic Drawing of The Engine Mounting



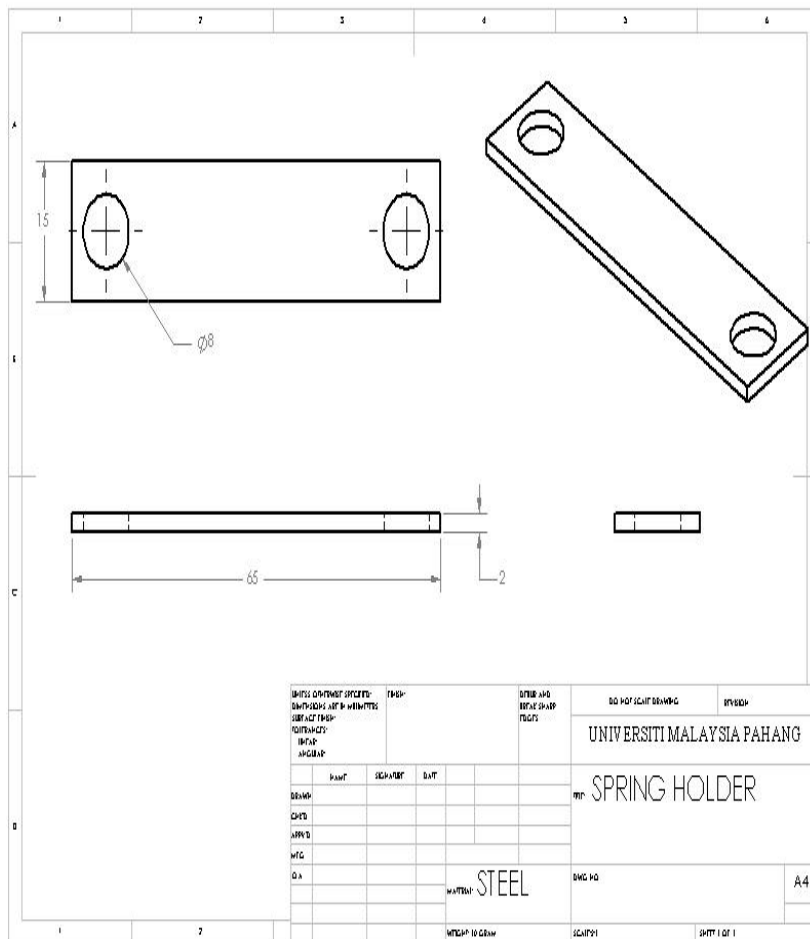
APPENDICE D5

The Ortographic Drawing of The Servo Holder



DRAFTSMAN: CHECKED: APPROVED: DATE:		TITLE AND REFERENCE: SERVO HOLDER	COURSE: DEPARTMENT: FACULTY:	UNIVERSITI MALAYSIA PAHANG
NAME: NO. DATE:	NAME: NO. DATE:	NAME: NO. DATE:	NAME: NO. DATE:	SERVO HOLDER
MATERIAL: WOOD			DWG NO:	SHEET: SHEET 1 OF 1

APPENDICE D6
The Ortographic Drawing of The Spring Holder



APPENDICE D7

The Ortographic Drawing of The Test Bed

